

Determination Of Lubricant Quality Using Maximum Bubble Pressure Method

by

Ishita Banerjee

A thesis submitted to the Graduate Faculty of
Auburn University
in partial fulfillment of the
requirements for the Degree of
Master of Science

Auburn, Alabama
August 9, 2010

Copyright 2010 by Ishita Banerjee

Approved by

Dong-Joo Kim, Chair, Associate Professor of Materials Engineering
Bryan A. Chin, Professor of Materials Engineering
Arnold Vainrub, Associate Professor of Anatomy, Physiology and Pharmacology

Abstract

A common lubricant in vehicles is Motor oil. Motor oil deteriorates in quality due to oxidation, thermal breakdown, micro-dieseling, additive depletion, electrostatic spark discharge or contamination. Reaction with oxygen causes spoilage of oil quality. Some effects of oxidation are an increase in viscosity, formation of a varnish, sludge, additive depletion and sediment formation.

During the movement of machinery through which fluids flow to keep the parts moving smoothly, heat is generated. This heat causes the oil temperature to increase. Overheating could damage the lubricant. Thermal breakdown can cause breakdown of additives, release of gases, production of insoluble substances. It could also result in a decrease in viscosity.

The degraded oil shows a major change in bubble interval. Surface tension may or may not change due to deterioration. Since, the effect of degradation of oil on surface tension is not that obvious. Hence, studying the changes in viscosity of fluid may prove to be more suitable to determine the quality of liquid.

Surface tension and viscosity are two properties of fluids that change due to deterioration. Among the many measurement methods, this research uses the Maximum bubble pressure method (MBPM) to study the dynamic surface tension in a liquid-gas interface. Here, a simple setup is proposed to study the two fluid properties. Nitrogen gas

is injected into different fluids of known surface tension. A new structure, in the form of “J” or inverted tube is suggested to ease the flow of bubbles after release.

Water and glycerin were first studied as their surface tension and viscosity values could be determined easily. By using equations found in the literature, the surface tension and correction factors were calculated. Viscosity was calculated in a similar manner. Since the pressure is measured at the top of the capillary tube instead of inside the bubble, and due to aerodynamic and viscosity effects, the pressure is higher than the actual value. The corrected surface tension, however was quite close to the correct values. Similar results were obtained for viscosity.

Clean motor oil, Valvoline 10W-30, and used motor oil of the same brand and grade were then studied. The surface tension was lower for the used oil as was the viscosity. The difference in viscosity was much higher than the difference in surface tension. Hence viscosity may be a better determining property for fluid degradation.

This thesis highlights some of the existing methods for measurement of surface tension in fluids such as water, glycerin, and oil. The merits and demerits of some of the techniques are listed. A new technique using a “J” tube, was developed during this research to measure surface tension in such fluids. Results presented in this research show the consistency of this technique for such measurements. This technique has the potential for application in measurement of surface tension and viscosity in vehicle engine oil, in extreme operating conditions.

Acknowledgements

The author would like to acknowledge the invaluable guidance and suggestions provided by Dr. Dong-Joo Kim, Professor of Materials Engineering and Dr. Bryan A.Chin, Chairman of the Materials Engineering program at Auburn University. Their valuable industrial experience and knowledge helped set the standards in performing and presenting research. Last, but definitely not the least, the author would like to acknowledge the “patience” and “encouragement” that friends and family exhibited during this endeavor.

Table Of Contents

Abstract.....	ii
Acknowledgements.....	iv
List of Tables	vii
List of Figures.....	viii
Chapter 1 Introduction	1
1.1 Overview.....	1
1.2 Thesis Structure	4
Chapter 2 Literature Survey.....	5
2.1 Surface Tension	5
2.2 Methods to determine surface tension in fluids.....	7
2.2.1 Du Noüy ring method	7
2.2.2 Wilhelmy plate method.....	7
2.2.3 Capillary rise method.....	8
2.2.4 Bubble Pressure Method.....	9
2.3 Available instruments	10
2.4 Viscosity	14
2.5 Fluid Degradation	16
Chapter 3 Experimental Details	17

3.1 Experimental Setup of Maximum Bubble Pressure Method	17
Chapter 4 Results and Discussion.....	24
4.1 Formulae and calculations	24
4.1.1 Volts to pressure conversion.....	26
4.1.2 Bubble time, bubble deadtime and bubble lifetime	27
4.1.3 Dynamic Surface tension	28
4.2 Fluids.....	33
4.2.1 Water.....	33
4.2.2 Glycerin.....	50
4.2.3 Motor Oil	52
Chapter 5 Conclusions	54
References.....	56
Appendix A: Correction Factors For Double-wall Tubes.....	59

List of Tables

Table 1 Commercially Available Tensiometers by Manufacturer.....	11
Table 2 Conditions tested out initially for water with capillary in the “straight” position. All flow rates are in sccm; 1,2,3,4,5	33
Table 3 Conditions tested out initially for water with capillary in the “inverted” position. All flow rates are in sccm; 1,2,3,4,5	34
Table 4 Bubble size dependence on various parameters	37
Table 5 Bubble Interval and frequency information for different flow rates	48
Table 6 Summary of the different parameters tested and their effects	49

List of Figures

Figure 1	Forces acting on different molecules in liquids	6
Figure 2	Surface tension acting on a surface	6
Figure 3	A Du Noüy ring tensiometer	7
Figure 4	Wilhelmy Plate method	8
Figure 5	Plot of pressure time during the bubble formation.....	9
Figure 6	Schematic diagram of a maximum bubble pressure tensiometer with a gas flow oscillation analyzer (BPA); 1 pump or compressor, 2,4 pneumatic volume, 3,5 capillaries, 6 differential pressure sensor, 7 pressure sensor, 8 internal gas volume of the instrument, 9 Peltier block, 10 valve, 11 measuring capillary, 12 PC-interface, 13 Computer[8].....	12
Figure 7	Bubble Pressure Method used by SITA proline f10[2].....	13
Figure 8	Bubble Pressure Method used by SITA proline f10[2].....	14
Figure 9	Graphical representation of the experimental Setup	18
Figure 10	Schematic of the capillary tube setup.....	18
Figure 11	Laboratory setup of the experiment with the capillary tube in “J” position.....	20
Figure 12	Double-walled angular tube and their structure	21
Figure 13	Double-walled tubes showing the outer diameter and inner diameter	21
Figure 14	Photograph of the capillary tube attached to the depth measuring system in a) “J” position and b) “Straight” position	22
Figure 15	Experimental arrangement for measuring motor oil readings.....	23
Figure 16	Signal from double-walled “J” tube of 30° angular tip and flow rate 2 sccm in water.....	25

Figure 17	Relation between volts and mm of water using a Baratron pressure transducer	26
Figure 18	Pressure Time dependence with bubble time t_b , bubble deadtime t_d and bubble lifetimes t_l as indicated.....	27
Figure 19	Bubble formation and relation to pressure [10] [17].....	28
Figure 20	a) Example of irregularity in waveform with a pressure transducer without an internal noise reduction circuitry b) Example of a waveform with a Baratron pressure transducer with an internal noise reduction circuitry	31
Figure 21	Max and min volts using a) a simple pressure sensor b) Baratron pressure transducer with an internal noise reduction circuitry, for the same tube	32
Figure 22a	Bubble Size vs. Inner diameter for double-walled “Straight” and “J” tubes of orifice angles 30°, 45° and 60°	35
Figure 22b	Relation between change in volts and internal diameter	35
Figure 23a	Dependence of bubble interval on depth for straight position tube with orifice angles of 30°, 45° and 60°	38
Figure 23b	Dependence of surface tension on depth for straight position tube with orifice angles of 30°, 45° and 60°	39
Figure 24	Effect of increasing depths on the a) Bubble Interval b) Offset voltage	40
Figure 24	Effect of increasing depths on the c) Change in volts	41
Figure 25a	“Straight” position: response of bubble interval to increasing flow rates	42
Figure 25b	“Straight” position: response of change in volts to increasing flow rates.....	42
Figure 25c	Relation between Flow rate and Surface Tension of a double-walled tube in “straight” position	43
Figure 26	Relation between change in pressure and Surface Tension.....	43
Figure 27a	Relation between surface tension and bubble lifetime	44
Figure 27b	Dependence of surface tension of pure water [8].....	45
Figure 28	Relation between flow rates and depths with change in voltage for double-walled tube of orifice angle of 0°	46

Figure 29	Bubble Interval Vs. Flow Rate for Straight and Inverted position for double-walled tube with an angle of 30° at the orifice	47
Figure 30	Relation between surface tension and bubble interval for “Straight” and “J” orientation	48
Figure 31	Relation between change in volts and the flow rate for glycerin using a double-walled “J” tube of orifice angle of 45°	52
Figure 32	Relation between dynamic surface tension (dyne/cm) and bubble lifetime(s) for glycerin using a double-walled “J” tube of orifice angle of 45°	52
Figure 33	Surface tension of clean and used Valvoline 10W30 motor oil	53
Figure 34	Viscosity of clean and used Valvoline 10W30 motor oil.....	54

Chapter 1 INTRODUCTION

1.1 Overview

Industrial fluids such as lubricants undergo degradation while in service, due to either normal or severe operating conditions. An ability to provide early detection of this degradation by measuring fluid properties would eliminate the possibility of mechanical failure resulting from lubricant breakdown. In turn, detection of fluid properties involves detection of surface tension and viscosity. Bubble Pressure method is chosen to detect this deterioration by simultaneous monitoring of surface tension and viscosity.

The molecules at the surface of a liquid only face attractive forces due to the molecules inside the liquid. This causes a tensile force to act on the surface, acting outward in the normal direction to the interior of the liquid. The surface tension causes the surface area to shrink. To increase the surface area, work has to be done. Presence of impurities, reduces the tensile force and the surface tension. This information is hence useful in studying the quality of various liquids. It has been used to study industrial fluids.

In 1851, Simon first proposed the “Maximum Bubble Pressure method” to measure the dynamic surface tension of liquids. This method worked well for smaller quantities and for a range of temperatures [1]. Experiments performed by various users showed differences in the results. Until then, it was assumed that there was a direct relationship between the surface tension and the pressure in the bubble. The error

introduced by usage of small tubes was much less and could be ignored. The method used played a major role in measurement of fluid properties. For example, when there is no contact between the liquid and the solid, the bubble pressure method is more accurate. Also, this method was being used with calibration done using a pure liquid like water. A larger radius is better as the thin film produced is almost flat. But this would require larger quantities of liquid and a larger container to house the entire setup, which is undesirable. Hence, smaller radii are preferred. Ever since, attempts have been made to modify and improve on this method.

The difficulties faced so far were overcome by the two-capillary method suggested by Sugden[1]. Two capillaries of two different radii are immersed to the same depth in the liquid and the surface tension can be accurately calculated from the difference in pressure in the bubbles formed by the two tubes. Fainerman conducted tests on this approach and concluded that the bubble formation frequency (lifetime) and the deadtime of the bubbles formed by the two tubes should be the same to get good surface tension results using Sugden's two capillary method [2]. In case of pure liquids, this method works successfully[3]. Other static excessive pressures are also eliminated, hence this method gives a strong relative signal.

According to the bubble pressure method, one capillary is introduced into the fluid. On flowing gas through this capillary tube, due to increasing pressure, bubbles are formed. The characteristics of the bubbles formed have been studied intensely. The maximum pressure difference is used to measure the surface tension of the liquid using the Laplace equation:

$$P - p = 2\gamma/r$$

where

p is hydrostatic pressure = ρgh .

ρ is the density of the liquid

h is the depth of the capillary from the surface

g is the gravitational force

γ is the surface tension

P is the measure pressure of the system

The surface tension, however is usually higher, due to the effect of viscosity and aerodynamic effects. A possible reason for this may be due to hydrophobic conditions on the outside of the tube [4][5]. Another reason may be the fluctuations in the atmospheric pressure around the system. The equation is hence modified to add the correction factors. Kovulchuk and Dukhin suggested the use of short and wide capillary as a solution to this problem[7][8].

The effect of gravity is reduced when an inverted capillary tube is used. Since fabrication of such a system is cumbersome, this research proposes a tube of a “J” or bent or “inverted” form. Comparison of readings taken in this position with data taken under similar conditions using a “vertical” position for the same tube proves that the “inverted” or “J” shaped tube arrangement is preferable.

The inverted capillary tube (or “J” shaped tube) assists in the rise of the bubble to the top by reducing the effects of buoyancy. By choosing the right surfactants to increase the wettability, this method can be applied in medicines, in studying the contamination in

oil or biological fluids, in printing etc. In vehicles, an oil sensor could be manufactured to indicate the oil quality and hence inform of the need for an oil change.

1.2 Thesis Structure

The contents of this thesis is divided into chapters. The first chapter contains an overview of this research and the thesis structure. The second chapter talks about the related literature and their contents. Properties of fluids studied in this research like surface tension and viscosity are discussed. Chapter three explains the details of the experimental setup. Chapter four discusses the results and discusses the details of the outcome of this research. The conclusions drawn from this research are summarized in the fifth chapter. The appendix contains some of the data from this experiment.

Chapter 2 LITERATURE SURVEY

2.1 Surface Tension

Surface tension is a fluid property. The molecules of a fluid experience attractive forces due to the surrounding molecules. Inside the fluid, a molecule is surrounded on all sides by other similar molecules, thereby making the net attraction equal to zero[1].

When such a particle is raised to the surface, the particle in the center is attracted downward by more liquid particles than in the upward direction as there are fewer air particles in the upward direction. The surface molecules experience an imbalance of attraction due to the presence of liquid molecules in the interior only. Hence, there is a net inward force acting on them. The surface molecule is unable to move down as it would need to squeeze out another particle onto the surface. Hence, this results in reduction of the surface area and the surface molecules form a stretched elastic membrane. To increase the surface area, work has to be done to overcome these forces[9].

A common example of this phenomena is observed when a dry brush is dipped into liquid. The hairs stick to each other as a surface film formed makes the hairs come closer. When the brush is dipped way inside a container of liquid however, it spreads out.

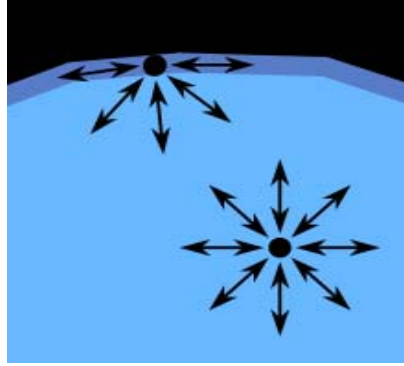


Figure 1: Forces acting on different molecules in liquids[9]

There exists a pressure difference on the two sides of the surface under tension. This pressure difference results in the surface tension and is given by the Young-Laplace equation of

$$\Delta p = \gamma \left(\frac{1}{R_x} + \frac{1}{R_y} \right)$$

where

Δp is the pressure difference

R_x and R_y are the radii of curvature in the two directions

γ is the surface tension

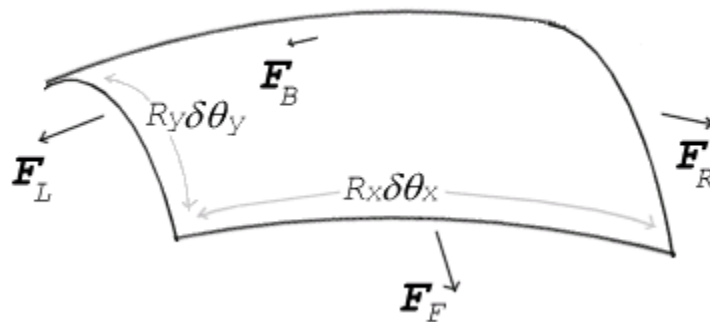


Figure 2: Surface tension acting on a surface [9]

Tensiometer is an instrument that can be used to measure the surface tension (γ) of liquids, with a pressure sensor at one end of a fluid filled tube. It is used to measure energy.

2.2 Methods to determine surface tension in fluids

Some commonly used methods of determining the surface tension are:

2.2.1 Du Noüy ring method

In 1925, Pierre Lecomte du Noüy proposed this method. A platinum ring or a metal needle with a small diameter is raised from the liquid being studied and the surface tension is calculated using the force required to raise it.

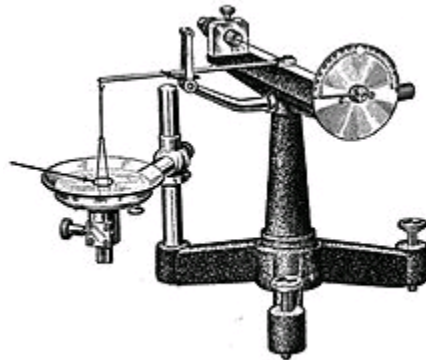


Figure 3: A Du Noüy ring tensiometer[9]

2.2.2 Wilhelmy plate method

A thin glass or platinum plate is inserted between the two interfaces and the force acting on it is measured[9].

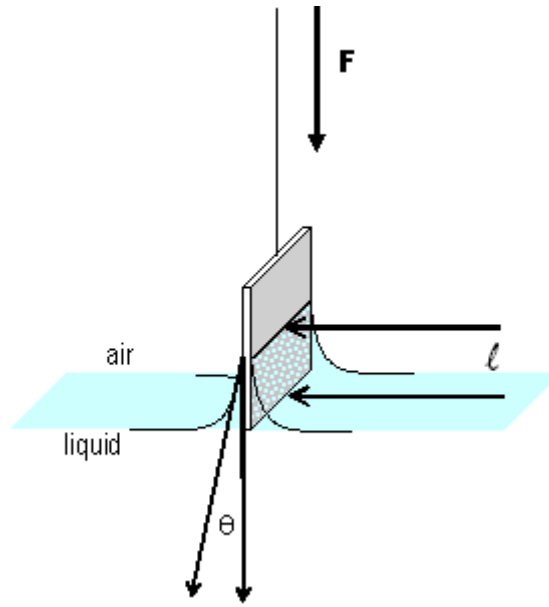


Figure 4: Wilhelmy Plate method[9]

2.2.3 Capillary rise method

Introduction of a capillary tube into a liquid causes the liquid to enter in the capillary. The height can be used to calculate the surface tension using the following formula:

$$h = \frac{2\gamma_{la} \cos \theta}{\rho g r}$$

- h is the height the liquid is lifted,
- γ_{la} is the liquid-air surface tension,
- ρ is the density of the liquid,
- r is the radius of the capillary,
- g is the acceleration due to gravity,
- θ is the angle of contact described above. Note that if θ is greater than 90° , as with mercury in a glass container, the liquid will be depressed rather than lifted.

2.2.4 Bubble Pressure Method

This method is usually used to study liquid-gas interfaces. It is used to measure the dynamic surface tension. The growth of bubbles formed dynamically in the liquid are studied in this method. The Laplace equation is used to calculate the dynamic surface tension:

$$\sigma = \frac{\Delta P_{max} \times R_{cap}}{2}$$

Where σ is the surface tension

ΔP_{max} is the maximum pressure difference

R_{cap} is the radius of the capillary

This method is usually used to study the presence of impurities.

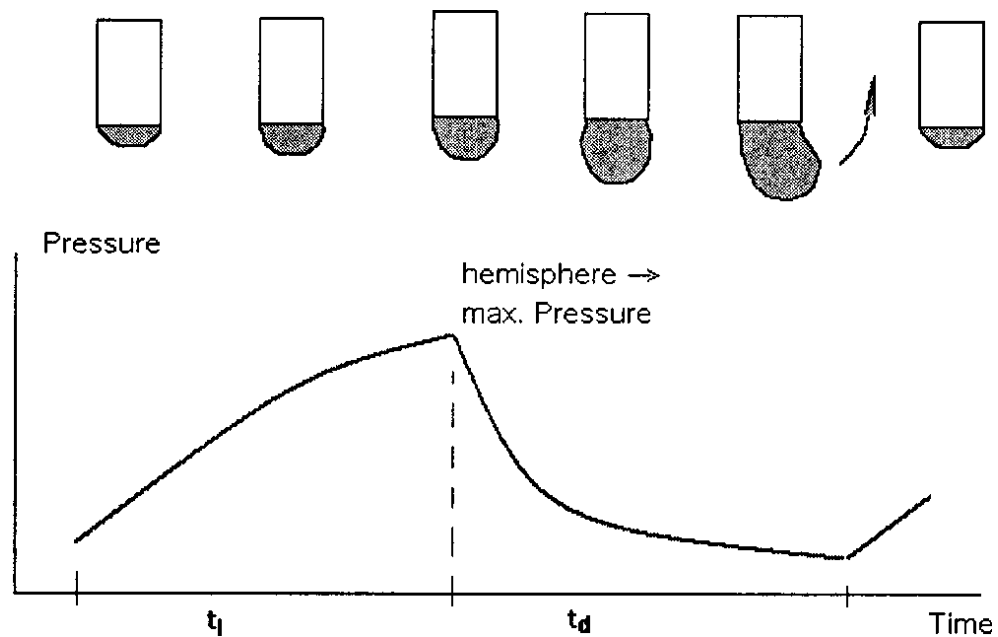


Figure 5: Plot of pressure time during the bubble formation [10]

2.3 Available instruments

The commercial instruments used to measure surface tension use capillaries of varying diameters. The methods of calculating surface tension also differ. Depending on the area of application, a particular instrument may be most effective. Some commercial tensiometers in the market are discussed below along with a brief description about their uses.

QBZY Series Full Automatic Surface / Interface Tensiometer is based on the Wilhelmy plate method. It is produced by Shanghai Fangrui Instrument Limited Company. The calibration is done using distilled water and ethanol. This method produces very accurate results while accounting for temperature effects. Below are listed some commercially available tensiometers.

Companies like Krüss, LAUDA, ChemDyne Research Corp., SINTERFACE and SITA all produce commercial tensiometers based on the Maximum Bubble Pressure method. The respective brands are listed in the table below. SensaDyne and SITA use small measuring systems with wide capillaries of 0.5 to 2 mm diameter[12]. The wide capillaries however reduce the accuracy of short adsorption times and hence these instruments are unsuitable for liquids with low surfactant concentrations.

Table 1: Commercially Available Tensiometers by Manufacturer

Manufacturer	Tensiometer Brand
Krüß	BP2
LAUDA	MPT2
ChemDyne Research Corp.	Sensadyn 5000
SINTERFACE	BPA
SITA Messtechnik GMBH	SITA

MPTc Lauda tensiometer is based on the Bubble Pressure method. It is fully automated, a small hand-held device with use anywhere and is user-friendly. It can measure dynamic surfactant tensions of low adsorption time range of below one millisecond to 20 seconds [11].

The BPA SINTERFACE tensiometer is also based on the bubble pressure method. Both the BPA and MPT2 use a large volume thus resulting in more accurate surface tension measurements.

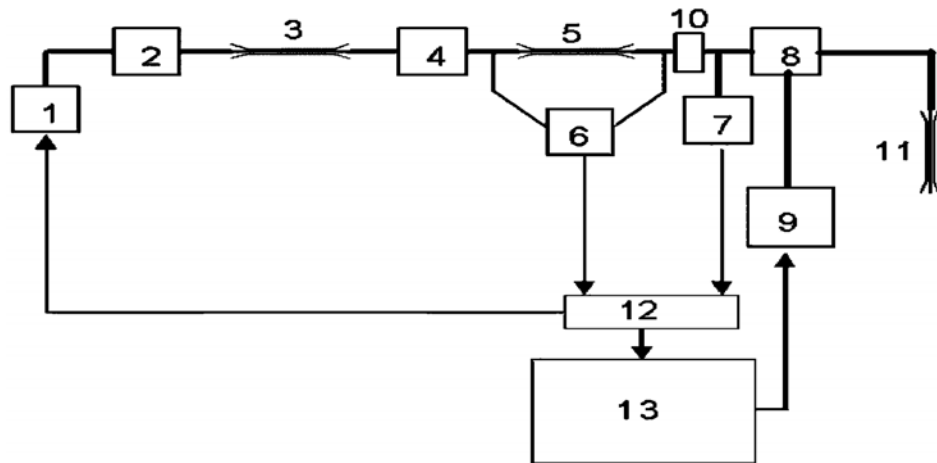


Figure 6: Schematic diagram of a maximum bubble pressure tensiometer with a gas flow oscillation analyzer (BPA); 1 pump or compressor, 2,4 pneumatic volume, 3,5 capillaries, 6 differential pressure sensor, 7 pressure sensor, 8 internal gas volume of the instrument, 9 Peltier block, 10 valve, 11 measuring capillary, 12 PC-interface, 13 Computer[4]

This tensiometer measures the lifetime and deadtime of the bubble accurately. The deadtime information can then be used to determine the correction factor of liquids with higher viscosity. Since the volume is large in this case, surface tension measurement is more precise. The same is the case with the MPT2 (Lauda) tensiometers. However, accounting for the hydrodynamic effects in the bubble time calculations is tedious. Fainerman, Makievski and Miller propose another method to do so using oscillations in the flow to determine the deadtime and lifetime of the bubble instead[10]. This also allows for using a larger volume.

The **SITA** method is useful for measuring the dynamic surface tension in aqueous solutions. This method is useful for measuring the concentration of surfactants since they reduce the surface tension of a solution. In the static

process, the surface being observed remains unchanged, while in the dynamic method, a new surface is created. Surface active molecules then attach to this surface.

The SITA proline f10 tensiometer uses the bubble pressure method, which is based on the time from the formation of the bubble to the point of maximum pressure in the bubble, as shown below.

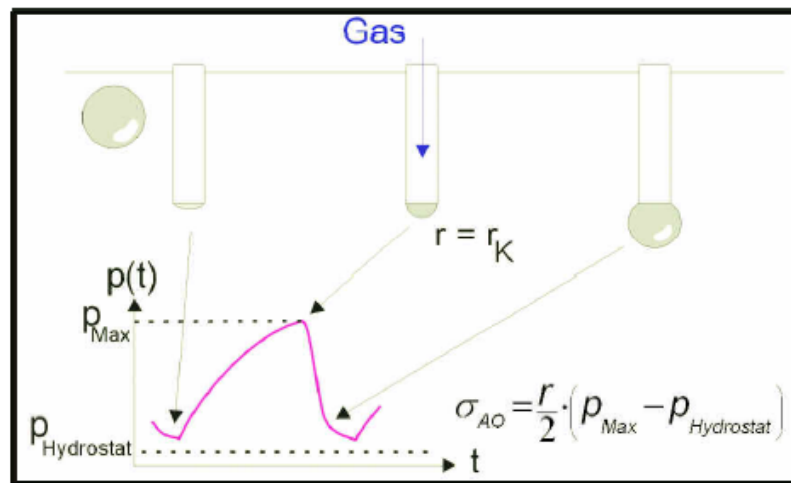


Figure 7: Bubble Pressure Method used by SITA proline f10[12]

The bubble pressure method can be automated. The SITA proline f10 tensiometer is suited for mobile use in production. The SITA scienceline t60 tensiometer is better suited for laboratory work, but can be used in the field as well. Below are some representative results that can be obtained with the SITA proline f10 tensiometer.

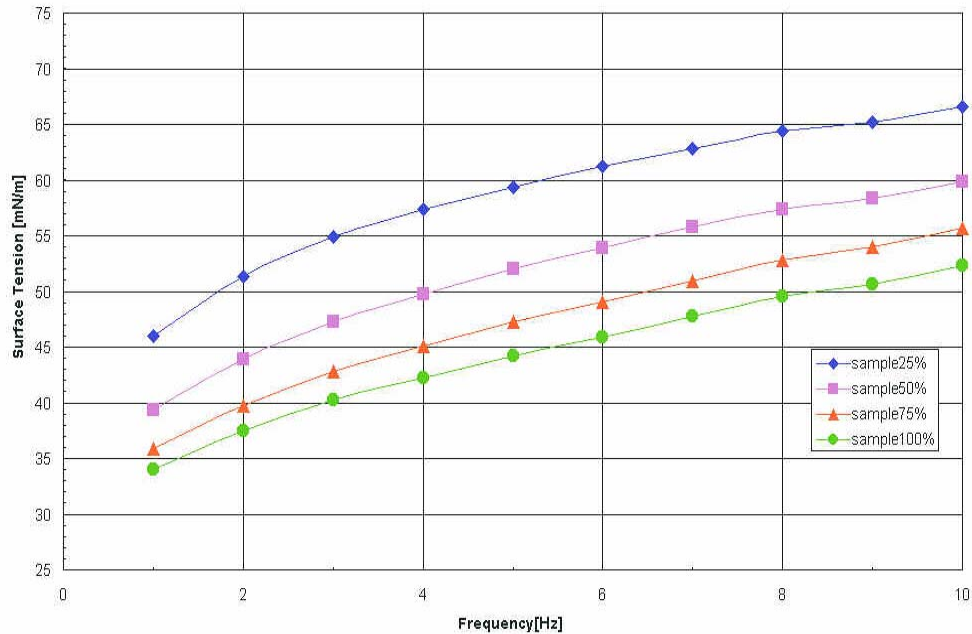


Figure 8: Bubble Pressure Method used by SITA proline f10[12]

2.4 Viscosity

Viscosity is yet another property of fluids of great importance in the study of fluids. Fluids can have varying concentrations. When a solid body is moved in a liquid by stirring or pouring, there is a resistance to the flow. This is due to the viscous nature of liquids. When there is a strong attractive force between a solid and a liquid, a layer of liquid coating is formed on the solid. i.e. the liquid is said to “wet” the solid, resulting in a layer of liquid to cling on to the solid surface. Also, there exists forces of attraction between liquid molecules. Any kind of motion between solid and liquid, as in stirring, or by the liquid movement, implies an attractive force exerted by the liquid layer attached to the solid on the adjacent liquid layers. Similarly, each subsequent layer exerts an attractive force on other layers. The layers, other than the one attached to the solid, get dragged along with the motion. Each

liquid layer subsequently drags other layers of liquid. The resistance to the motion is hence due to the layer attached to the solid and the other liquid layers.

One liquid can be more viscous than another. For example, water is less viscous than glycerin, which in turn may have a lower viscosity than oil.

Viscosity also increases with cold temperatures. Hence, in summer, the motor oils used are less viscous than in winter.

Viscosity therefore depends on the force to be applied on the layers of liquid to set them in motion at a certain velocity between the layers. It is found to be directly proportional to the velocity gradient and the area, when the two contiguous areas are of same area, through which the liquid is made to flow.

$$F \propto Ga ; F = nGa$$

where F is the force

G is the velocity gradient

a is the area when the area of each surface is the same

n is the coefficient of viscosity

Measurement of coefficient of viscosity to determine the viscosity of fluids is a hard task. A more common method used is to compare the viscosities of two liquids. The Sensadyne tensiometer uses the following equation to calculate viscosity of fluids with a known surface tension value:

$$\Delta\gamma = 3\eta r/2B_1$$

where

γ is the surface tension

η is the viscosity

r is the radius of the capillary tube orifice

B_1 is the bubble lifetime

2.5. Fluid Degradation

Over time, usage of fluids or lubricants in machinery can lead to their degradation. A common lubricant in vehicles is Motor oil. Oil can show deterioration in quality due to oxidation, thermal breakdown, micro-dieseling, additive depletion, electrostatic spark discharge or contamination [13]. Reaction with oxygen causes spoilage of oil quality. Some effects of oxidation are an increase in viscosity, formation of a varnish, sludge, additive depletion and sediment formation.

During the movement of machinery through which fluids flow to keep the parts moving smoothly, heat is generated. This heat heats up the oil. Overheating could damage the lubricant. Thermal breakdown can cause breakdown of additives, release of gases, production of insoluble substances. It could also result in a decrease in viscosity.

Surface tension may or may not change due to deterioration. The degraded oil shows a major change in bubble interval. Since, the effect of degradation of oil on surface tension is not that obvious. Hence, studying the changes in viscosity of fluid with known surface tension value may prove to be more suitable to determine the quality of liquid.

Chapter 3 EXPERIMENTAL DETAILS

Of the different surface tension measurement techniques mentioned in the previous section, the maximum bubble pressure method was chosen. The actual experimental details of the setup used in this research are listed below.

3.1. Experimental Setup of Maximum Bubble Pressure Method

The Maximum Bubble Pressure method (MBPM) is used to measure surface tension of liquids with a short time range typically less than a second.

A simple setup of this system would consist of a gas-flow system, a pressure sensor, a capillary holder, a capillary tube, liquid container, depth measuring system and a data acquisition system to convert the signal and store the data in a computer. An oscilloscope may also be used in parallel to view the signal and for verification of data.

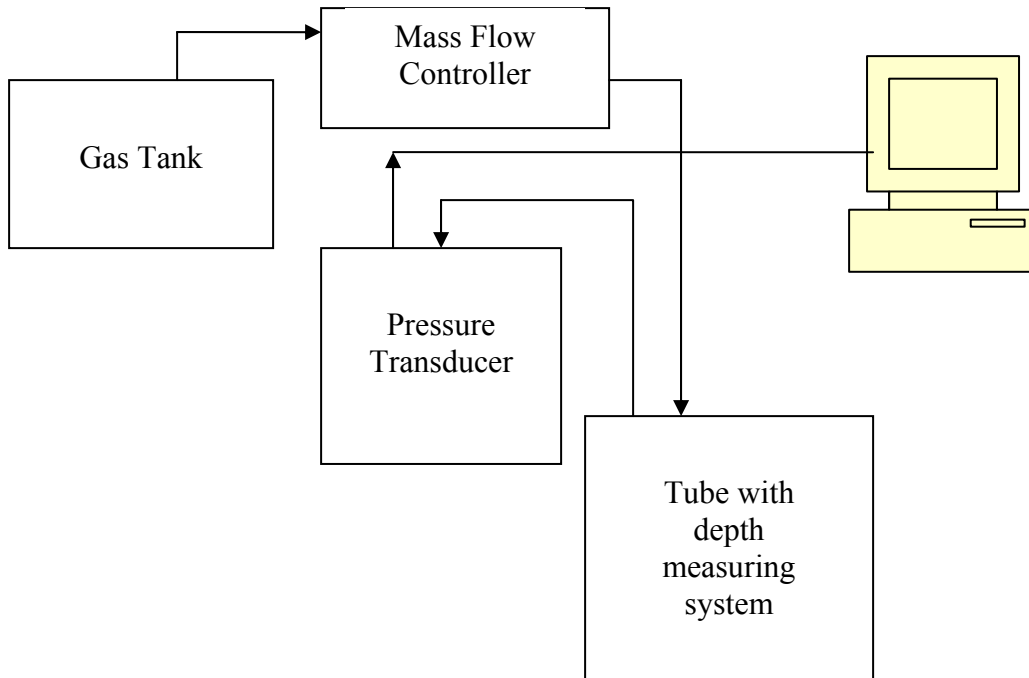


Figure 9: Graphical representation of the experimental Setup

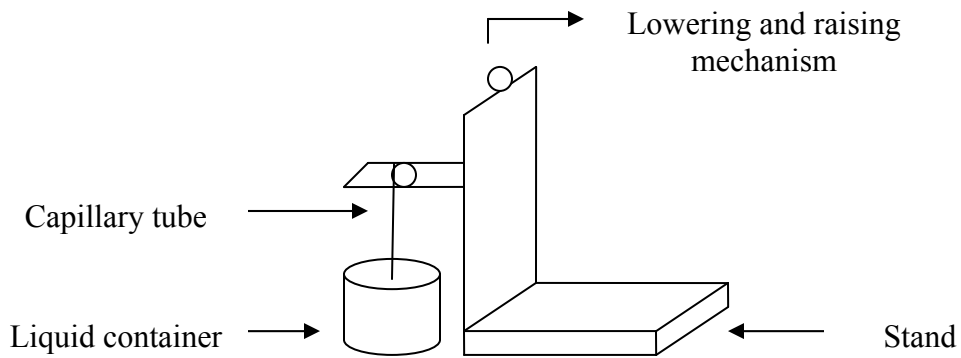


Figure 10: Schematic of the capillary tube setup

The setup in our experiment was as shown in the above figures. A Nitrogen cylinder containing compressed Nitrogen gas from Airgas company was used. This was connected directly to a rotometer or Porter VCD 1000 mass flow controller. The output of the rotometer was then connected to the vertical capillary holder setup attached with a digital vernier caliper for precise depth measurements. The arm of this setup was connected to the capillary tube. This arrangement allowed for more freedom of the kind of capillary tube to be used. Both the “vertical” position of the capillary and the “J” position of the capillary tube could now be setup easily. The pressure was measured at the upper end of the capillary with the help of a pressure sensor and the mass flow controllers attached to the line helped regulate the flow rate. A connection was made from the output of the pressure transducer to read the data using a data acquisition system, DATAQ DI-158U. The DI-158U was connected to the computer to retrieve the data and work off of it.

With this arrangement, the bubble intervals were quite irregular. This may be due to the hydrophobic nature of the outer side of the tube or due to the atmospheric fluctuations in the lab [4,5]. Using another pressure sensor Baratron Pressure Transducer 223BD 00010 A A US, used in the SensaDyne instrument, however provided a clean signal. Due to the in-built circuitry in the transducer for noise reduction, the results were good. With this small change, the bubble interval seemed to be very stable thereafter. The rotometer was now used to read the flow along with the mass flow controller.

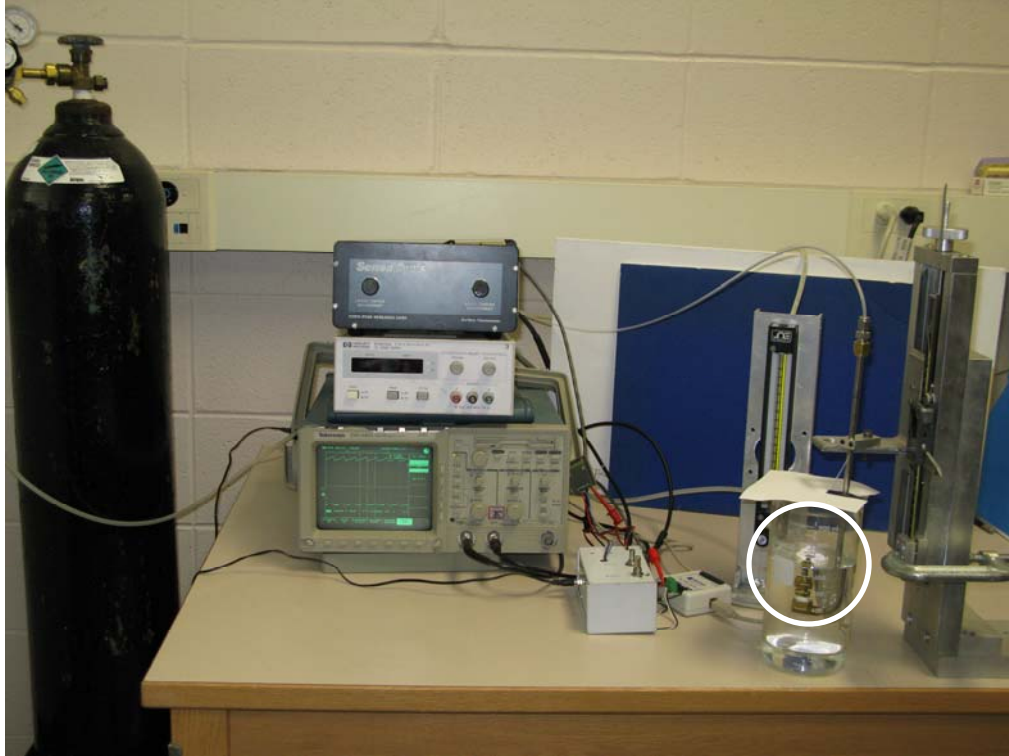


Figure 11: Laboratory setup of the experiment with the capillary tube in “J” position

Using the above setup, Nitrogen gas was made to flow through a capillary fitted with a pressure sensor on one end of the capillary. The other end was dipped into the liquid of interest, viz. water. The flow rate of the gas was varied using the mass flow controller and noted. The bubble size approximately ranged from 1mm to 4mm for a flow of 1sccm to 5sccm of N_2 gas in water. The readings were taken for a set of five depths of 1, 2, 3, 4 and 5mm for each flow rate through each capillary. This was done by using a digital vernier caliper attached to the board lowering the tube, to precise depths.

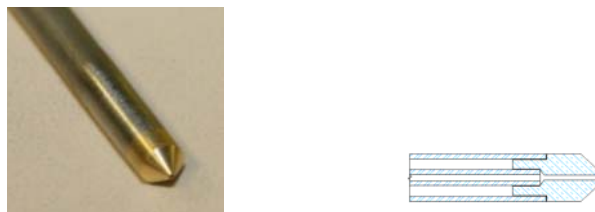


Figure 12: Double-walled angular tube and their structure

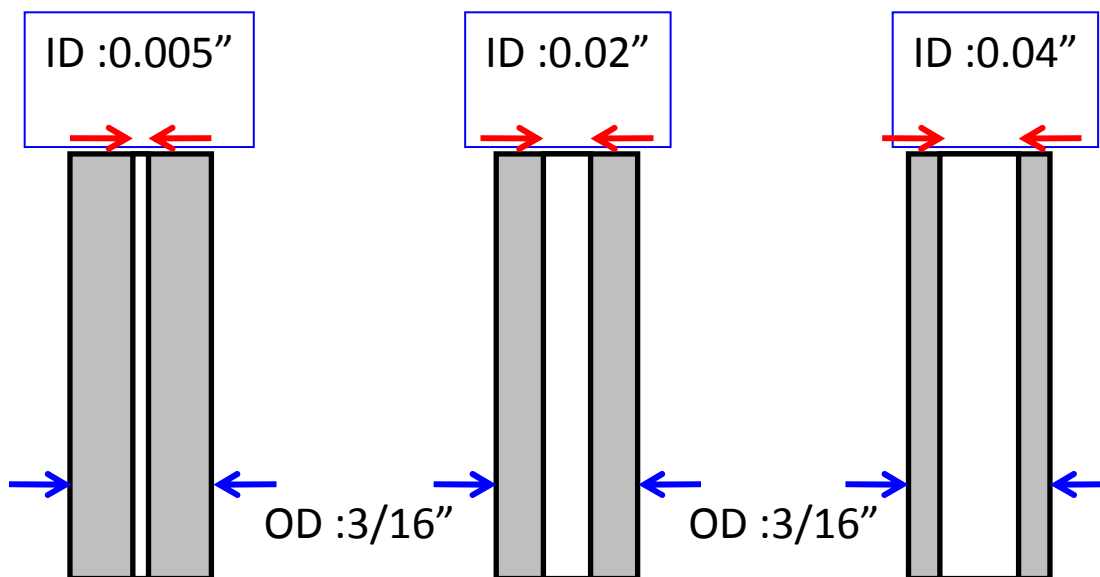


Figure 13: Double-walled tubes showing the outer diameter and inner diameter

Electrochemically etched steel capillary tubes of varying inner and outer diameters were considered and the results from the “vertical” or “straight” position and the “J” or “inverted” tube position were noted for each condition.

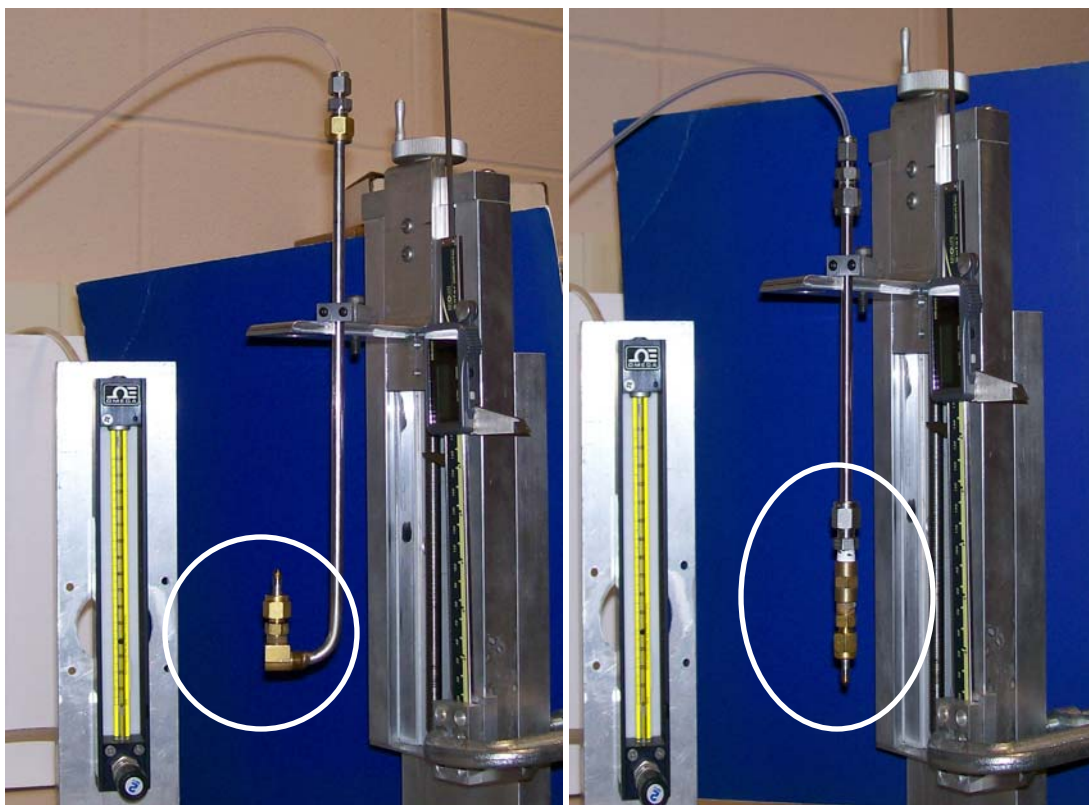


Figure 14: Photograph of the capillary tube attached to the depth measuring system in
a) “J” position and b) “Straight” position

Double-walled tubes had a constant outer diameter of 0.1875” or 3/16” and an inner metal tube with varying orifice sizes. Different geometries such as with a flat-bottom or 0 degrees or different angles of 30, 45 and 60 degree tips, were also used. Figures 12 and 13 show the construction of the double-walled tubes. Radii of the capillary tubes ranged from 0.01” to 0.04”. DI water was used as reference. Using a similar setup, readings were taken for other fluids of known surface tension as well.

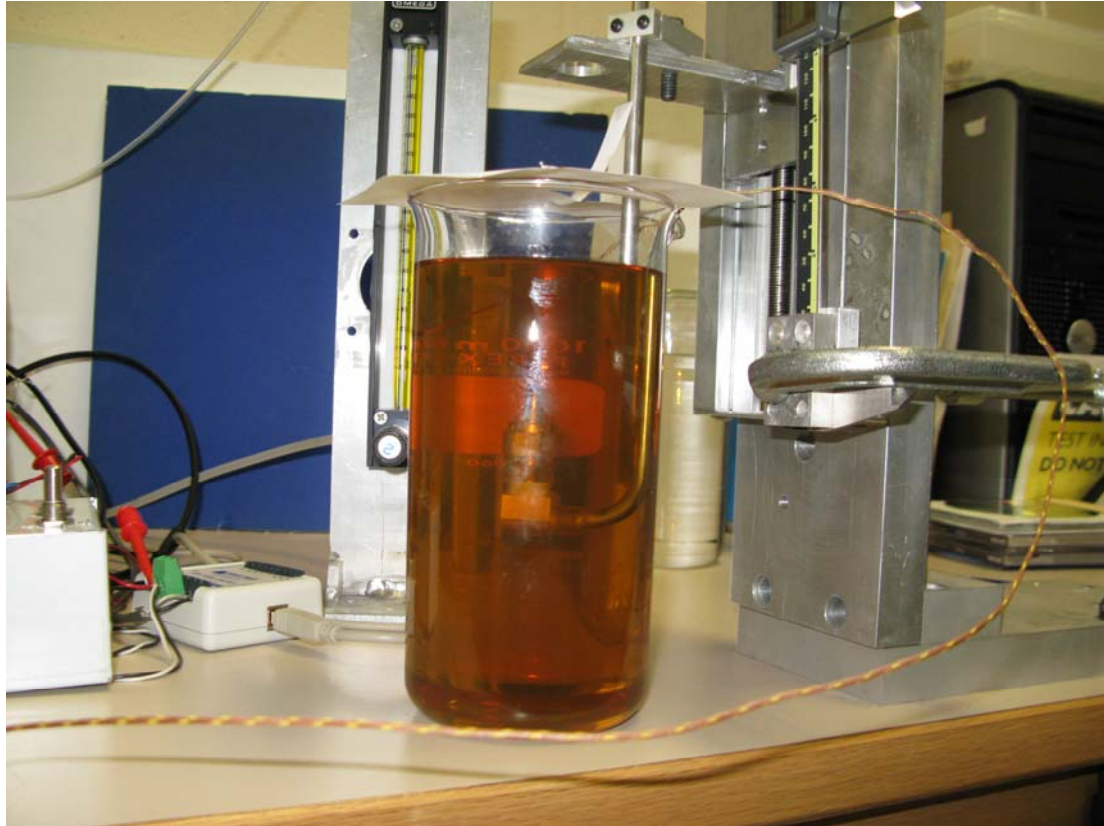


Figure 15: Experimental arrangement for measuring motor oil readings

A plot of pressure vs. time was recorded from the data acquisition system DATAQ or the oscilloscope. All experiments were conducted at room temperature. Analysis of the various contributing factors was done thereafter.

Chapter 4 RESULTS AND DISCUSSION

4.1 Formulae and calculations

The measurement procedure involved recording the data off of the oscilloscope or from the waveform files on the computer being used. These waveforms are used to determine the pressure as a function of the bubble rate at time intervals of one second or less depending on the sampling rate set up on the DATAQ. Figure 16 shows examples of the plots of volts and pressure as a function of time, generated using the data from the DATAQ. In figures 16 and 17, the output signal for water was obtained from the double-walled tube with an angle of 30° , in the “J” position for a flow rate of 2 sccm.

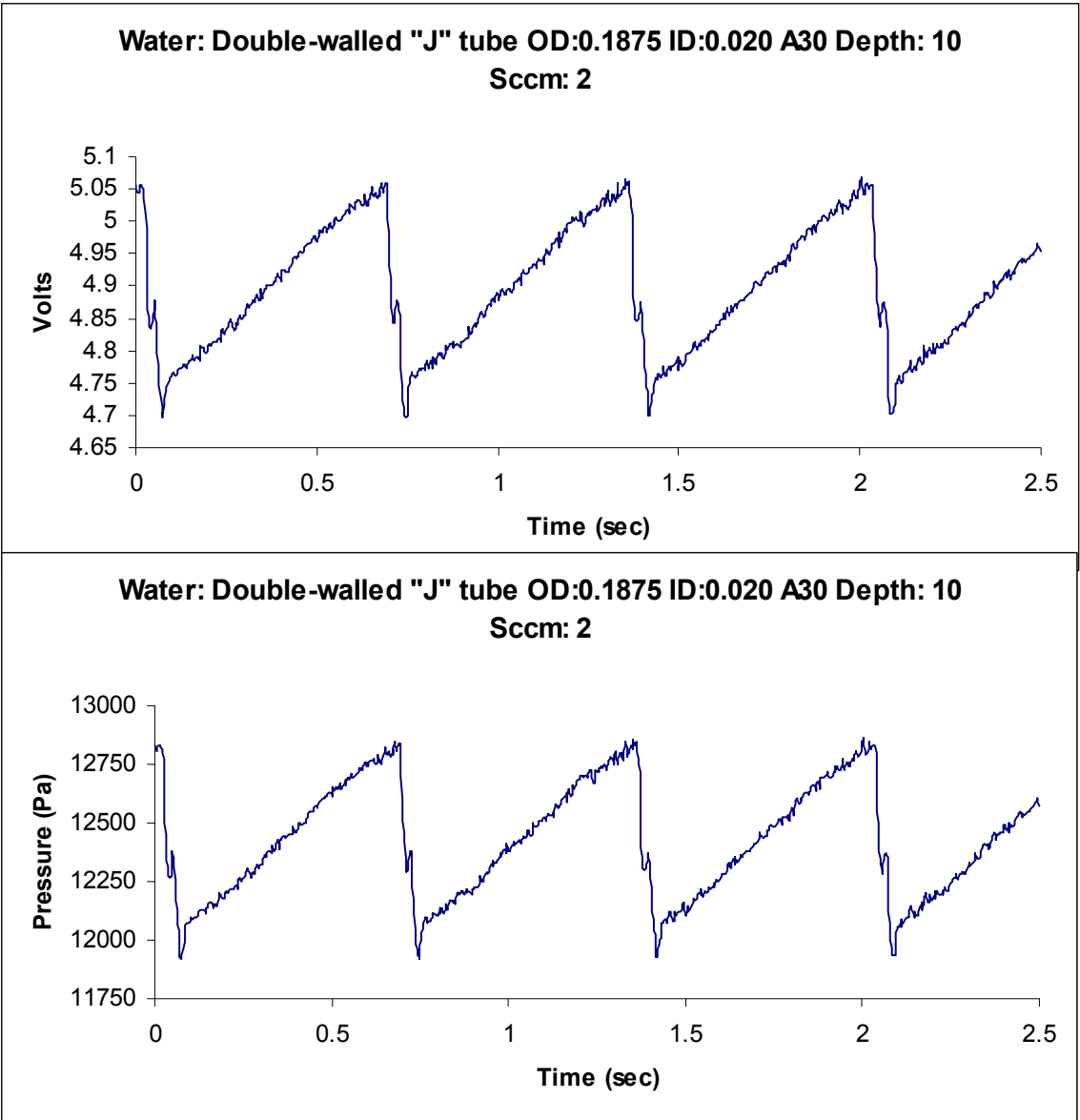


Figure 16: Signal from double-walled “J” tube of 30° angular tip and flow rate 2 sccm in water

4.1.1. Volts to pressure conversion

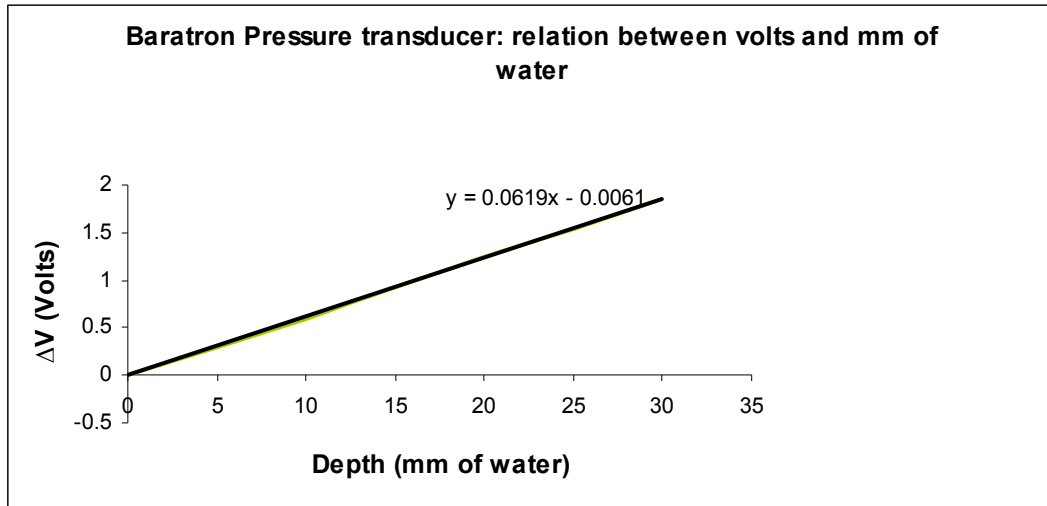


Figure 17: Relation between volts and mm of water using a Baratron pressure transducer

For the Baratron pressure transducer 223BD 00010 A A U S, figure 17 gives the relation between the measured voltage and the depth of water. The conversion from volts to pressure is then done as follows:

$$y \text{ (volts)} = (0.0619 * (x \text{ mm of water})) - 0.0061$$

$$1\text{mm of water} = 9.80665 \text{ Pascals [14]}$$

$$\text{Therefore, } x \text{ (Pa)} = (y + 0.0061) * (9.80665 / 0.0619) \dots\dots\dots(1)$$

by using the data in figure 16, and the above formula,

$$\Delta V = 0.37310 \text{ then}$$

$$\begin{aligned} \text{Change in pressure } \Delta P &= (\Delta V + 0.0061) * (9.80665 / 0.0619) \\ &= 961.2101 \text{ (Pa)} \end{aligned}$$

4.1.2. Bubble time, bubble deadtime and bubble lifetime

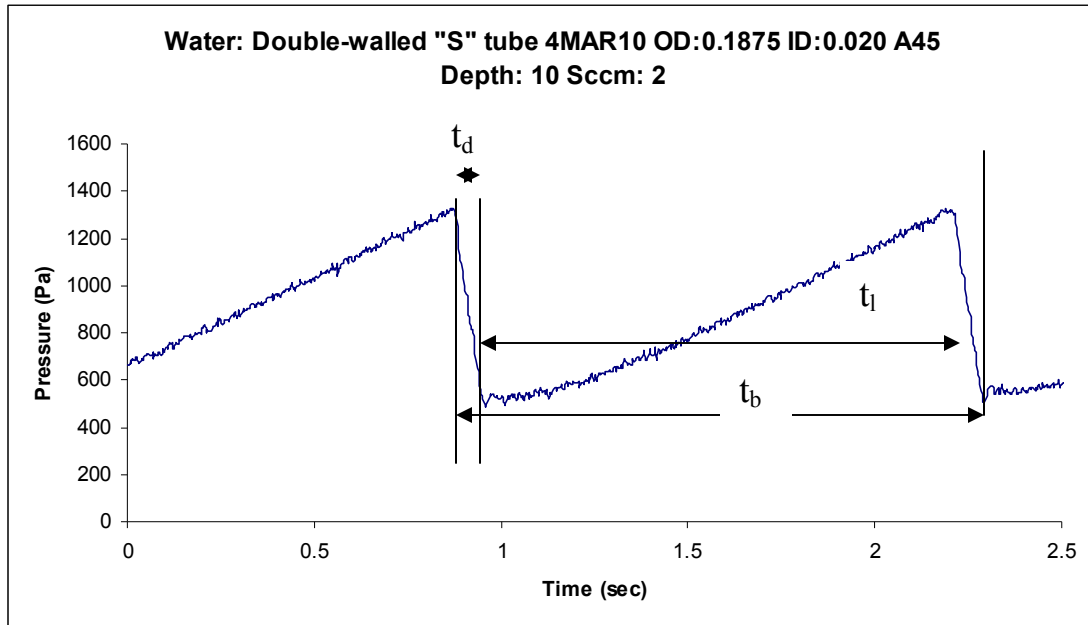


Figure 18: Pressure Time dependence with bubble time t_b , bubble deadtime t_d and bubble lifetimes t_l as indicated

Figure 18 shows how the bubble time, bubble deadtime and the bubble lifetime is determined from the plots. The total time taken in forming a bubble is the time period between one rise in waveform and the consecutive rise in the waveform or two minima in the waveform and is denoted by t_b , bubble time. The time marked by a decrease in pressure in the system and increase in flow, as seen in figure 18, is known as the deadtime t_d of the bubble. The time interval during which the pressure rises again and reaches a maximum, is known as the lifetime t_l of the bubble. The total bubble time is the sum of these two times. Using the following equation,

$$t_b = t_l + t_d \quad (2)$$

the lifetime and deadtime values can be calculated.

Figure 19 shows the dependency of pressure and the different stages that a bubble goes through during bubble growth.

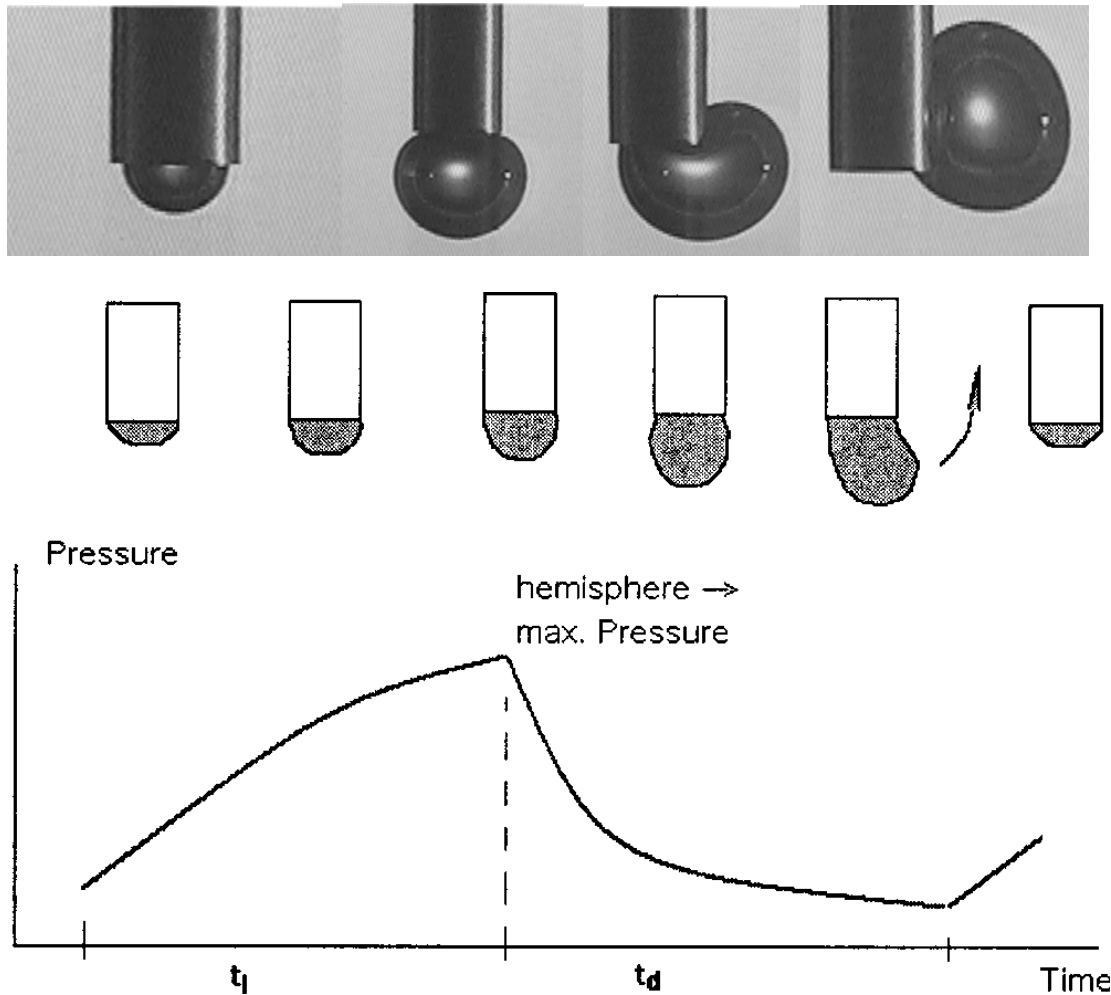


Figure 19: Bubble formation and relation to pressure [15][16]

4.1.3. Dynamic Surface tension

The maximum pressure is calculated using the maximum value of pressure in the graphs, averaged over a number of points. Similarly, the minimum pressure can be calculated from the minimum values on the waveform. The difference between the maximum and minimum pressure gives the pressure difference ΔP . Hydrostatic pressure

is computed by measuring the immersion depth in these experiments. The immersion depth has to exceed the bubble diameter to allow fast separation of the bubble from the capillary tip. The pressure at a depth of h is given by the hydrostatic pressure $P = \rho gh$ where g is gravitational acceleration and ρ is the density of the liquid. The dynamic nature of the bubbles gives rise to an increase in the measured pressure due to aerodynamic resistance of the capillary and the viscosity of the liquid. Since the interface here is a gas-liquid interface, the hydrostatic pressure is $P_h = \Delta \rho gh$. The real pressure P is then equal to the system pressure P_s without the excess pressure due to the dynamic effects P_d .

$$P = P_s - P_h - P_d \quad (3)$$

The surface tension is then calculated by substituting the maximum pressure and the radius of the capillary in the Laplace equation:

$$\gamma = f (P * R_{cap})/2 \quad (4)$$

where, f is the correction factor associated with the higher value of surface tension γ . The correction factor f is required for capillaries with a radius greater than 0.1mm. Since most of the capillaries in our experiment were of a bigger radius, the correction factor was calculated for each one. This takes care of the correction for non-spherical bubble shape which is usually associated with capillary tubes with a radius greater than 0.1mm [8]. Using water as reference liquid, the correction factor was calculated, using the known surface tension at the temperature at which the experiments were conducted. From equations (3) and (4), we then get

$$\gamma = [f (P_s - P_h) * R_{cap}]/2 - \Delta \gamma_a - \Delta \gamma_d \quad (5)$$

where, $\Delta \gamma_a$ is the effect due to the aerodynamic resistance and $\Delta \gamma_d$ is due to the viscosity of the liquid [8].

For example, calculation of surface tension of water of known surface tension of 71.97 dyne/cm, with radius = 0.025cm and $\Delta P = 961.2101$ Pa, would be as follows:

$$\begin{aligned}\text{Measured surface tension } \gamma &= f (\Delta P * R_{cap})/2 \\ &= [961.2101 * 0.025]/2] * 10 \text{ dyne/cm} \\ &= f[120.1513] \text{ dyne/cm} \\ \text{Correction factor } f &= 71.97/120.1513 \\ &= 0.598995\end{aligned}$$

Using a pressure sensor with no internal circuitry for noise reduction led to signals with a lot of irregularity, as seen in figure 20a. Some of the irregularity could be attributed to the oscillations resulting at the instant a bubble begins to form due to changes in the pressure at the two ends of the capillary. The capillary tubes used in experiments presented in this research, were made of electrochemically etched steel on both the inner and outer surfaces. Another possible reason may be due to absence of internal noise reduction circuitry. The Baratron pressure transducer from MKS instruments, Model # 223BD_00010AA US, has an in-built noise reduction circuitry, which produced clean signals. Using this transducer, the minimum voltage measured was constant. Hence, the results reported were done using the Baratron pressure transducer.

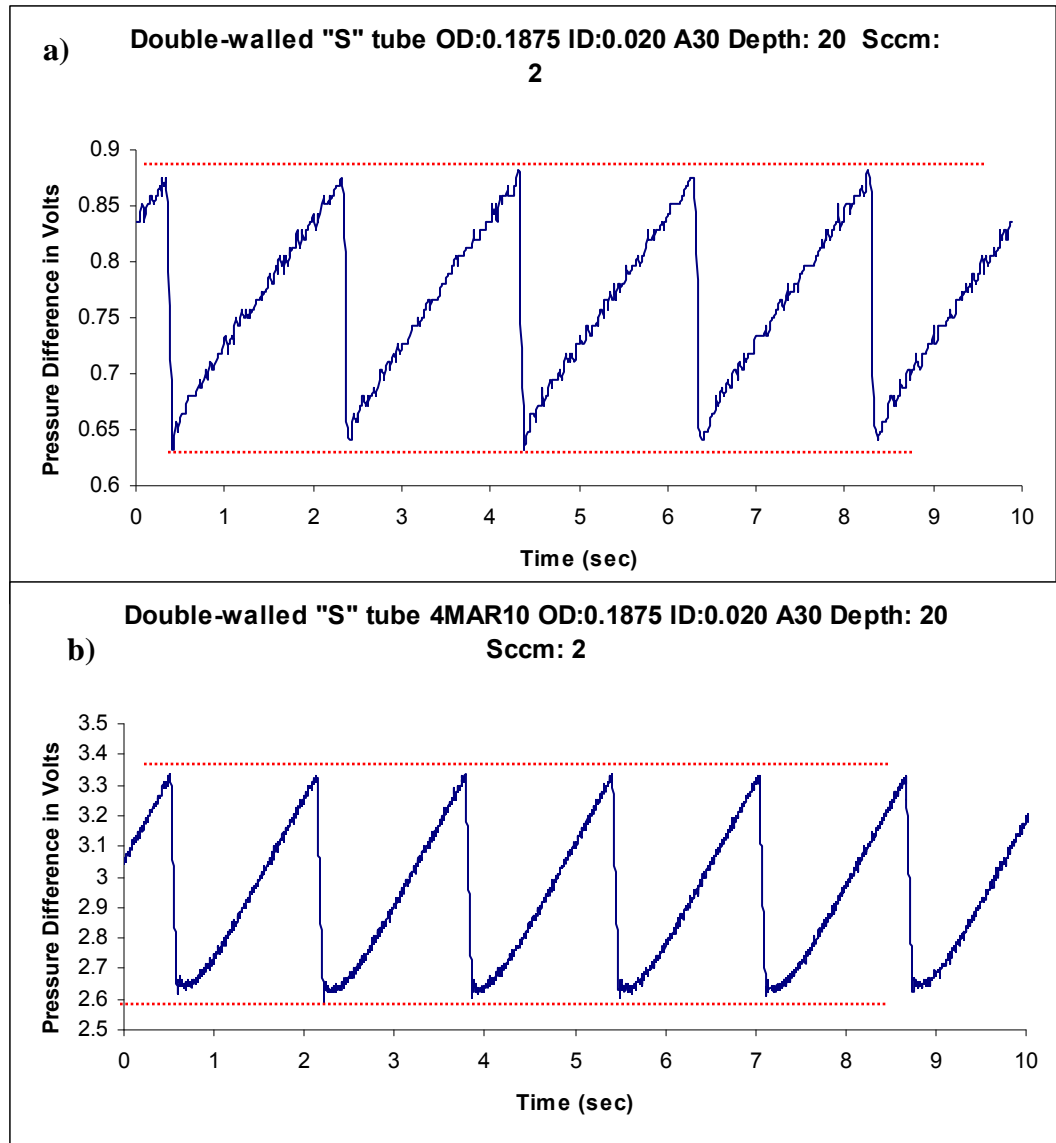


Figure 20: a) Example of irregularity in waveform with a pressure transducer without an internal noise reduction circuitry b) Example of a waveform with a Baratron pressure transducer with an internal noise reduction circuitry

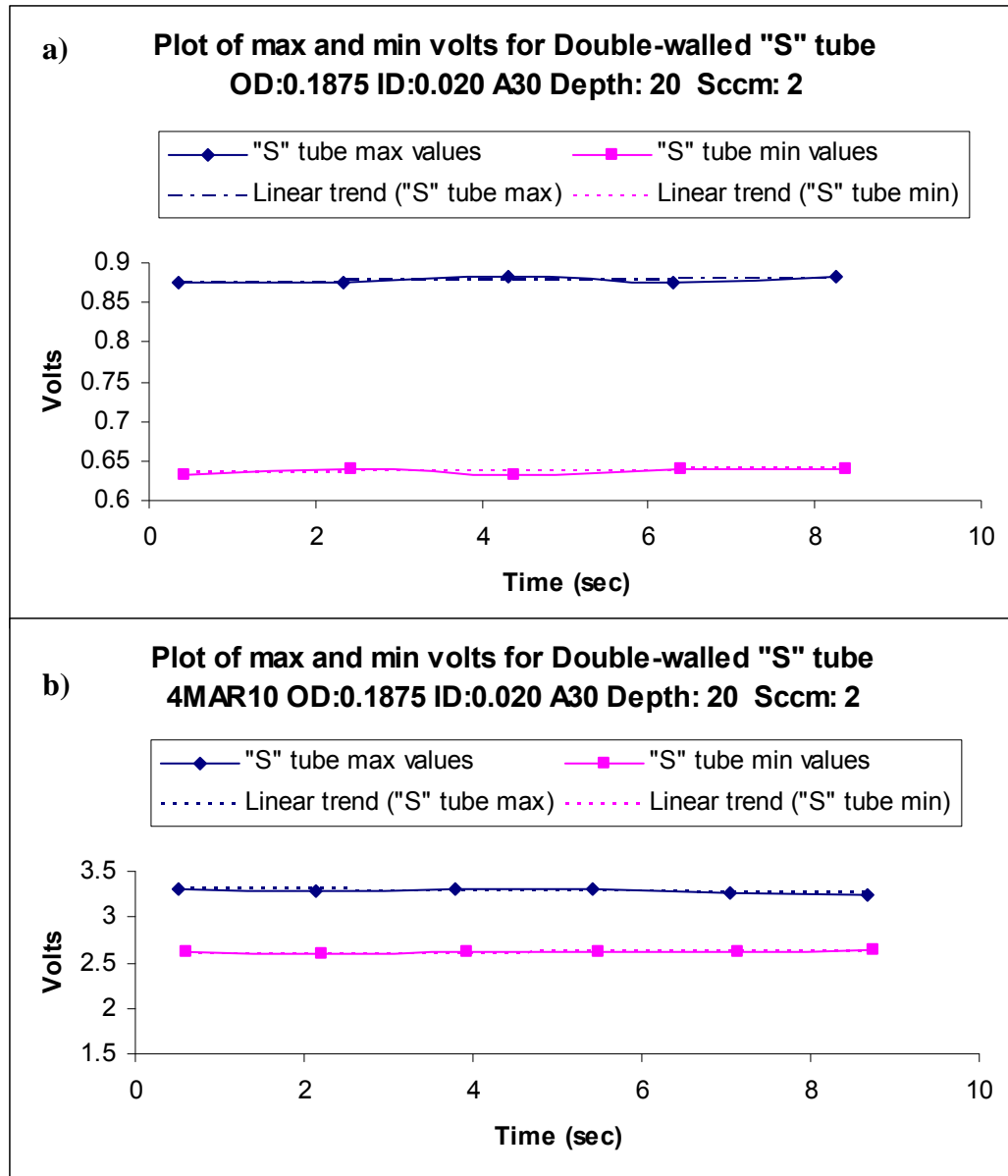


Figure 21: Max and min volts using a) a simple pressure sensor b) Baratron pressure transducer with an internal noise reduction circuitry, for the same tube

As the pressure transducer was attached to the tip of the capillary at the top end, the measured pressure was expected to be higher than in the bubble itself. Since the area of interest is the pressure inside the bubble, gravitational and aerodynamic effects have to

be accounted for. The correction factor is important information required in calculation of surface tension for other highly viscous liquids.

4.2 Fluids

Tests were run for three different fluids of known surface tension at room temperature: water, glycerin, and motor oil. Of these, water had the lowest viscosity and glycerin the highest. The results were as listed below:

4.2.1 Water

Parameters like the internal diameter (ID) of the capillary tube, outer diameter (OD) or single-walled (SW) / Double-walled (DW), depth, flow rate in sccm, angle of orifice (0°, 30°, 45°, 60°) were tested. The table below lists the different conditions tested and measurements done with the capillary tube in the “straight” position.

Table 2: Conditions tested out initially for water with capillary in the “straight” position.

All flow rates are in sccm; 1,2,3,4,5

ID	Single-Walled			Double-Walled			
	OD			OD			
	1/32" 0.03125"	1/16" 0.0625"	1/8" 0.1250"	Angle			
			0°	30°	45°	60°	
0.005				1,2,3,4,5			
0.010	3			1,2,3,4,5			
0.020	3	1,2,3,4,5		1,2,3,4,5	2,3		2,3
0.030		1,2,3,4,5		1,2,3,4,5			
0.040		1,2,3,4,5		1,2,3,4,5			

Table 3: Conditions tested out initially for water with capillary in the “inverted” position.

All flow rates are in sccm; 1,2,3,4,5

ID	Single-Walled			Double-Walled			
	OD			OD			
	1/32” 0.03125”	1/16” 0.0625”	1/8” 0.1250”	3/16” 0.1875”			
				Angle			
				0°	30°	45°	60°
0.005				2,3,4,5			
0.010	1,2,3,4,5			1,2,3,4,5			
0.020	2,3			2,3	1,2,3,4,5	2,3,4,5	1,2,3,4,5
0.030		1,2,3,4,5	2,3,4,5	2,3			
0.040		1,2,3,4,5		2,3,4,5			

Table 3 lists the different conditions tested out with a new orientation of the capillary tube in the “J” or “inverted” position. This position was expected to show less restriction in the rise of the bubble to the top of the liquid.

Internal Diameter

Tubes of internal diameter of 0.005”, 0.01”, 0.02”, 0.03” and 0.04” were tested. Of these, acquiring a good signal for 0.005” orifice was very difficult. These tubes were also susceptible to clogging up very easily. Hence, analysis with the tubes of larger diameters were preferred. It is hypothesized that the bubble size is dependent on internal diameter of the capillary initially. The bubble grows thereafter and extends to the outer diameter of the tube and is hence dependent on the outer diameter once maximum pressure is reached. Also, with increase in internal diameter, the change in volts should

increase. Figure 22a shows that the bubble size is constant for double-walled tubes in each orientation and figure 22b shows the change in volts

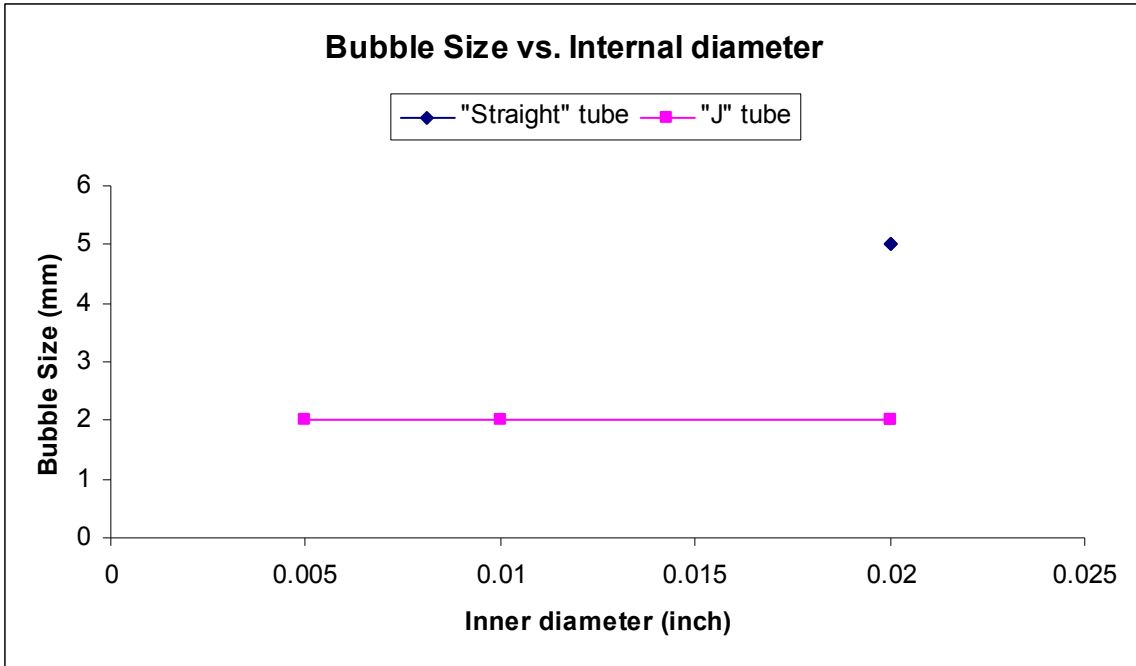


Figure 22a: Bubble Size vs. Inner diameter for double-walled “Straight” and “J” tubes of orifice angles 30°, 45° and 60°

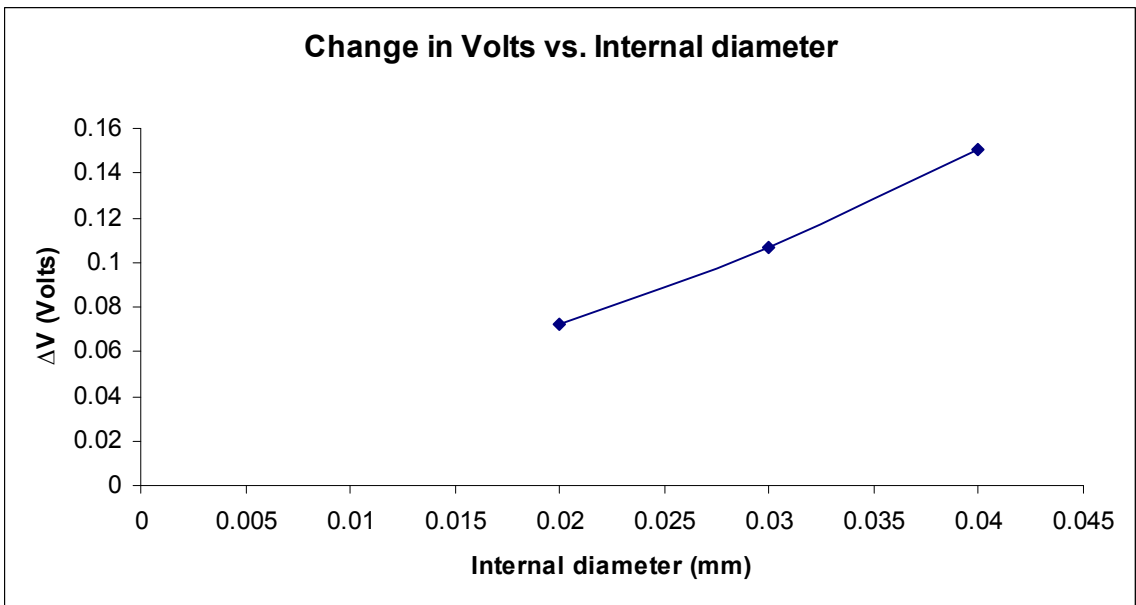


Figure 22b: Relation between change in volts and internal diameter

The experimental results are in agreement with the expected results.

Outer Diameter

Single-walled tubes had a smaller outer diameter than double-walled tubes. There were three outer diameters considered for single-walled tubes: $\frac{1}{8}$ " or 0.1250", $\frac{1}{16}$ " or 0.0625" and $\frac{1}{32}$ " or 0.03125". All single-walled tubes were flat at the base i.e orifice angle was equal to 0° . Double-walled tubes had a constant outer diameter of $\frac{3}{16}$ " or 0.1875".. The inner diameter for all these double-walled tubes was 0.02" or 0.51mm. The angle at the tip was varied. The double-walled tubes were designed as shown in the figures 12 and 13.

The size of the bubble depends on the outer diameter. It is hypothesized that with increase in outer diameter, the bubble rate will decrease. In the "straight" position, the bubble size should be smaller as it flattens out while in the "J" position, the bubble size should be larger as it stretches out freely. Also, the bubble interval for both smaller inner diameter and outer diameter should be small. i.e. the bubble frequency should be larger.

The results from this research are as given in table 4. The bubble size was determined by estimating the size of the rising bubble by sight. For example, for the double-walled tube of 0.02" inner diameter, and outer diameter 0.1875", in the "straight" position, the bubble size was 5mm while for double-walled tube of 0.02" inner diameter and outer diameter of 0.1875" in the "J" position, the bubble size was 2mm.

Table 4: Bubble size dependence on various parameters

No.	Inner Diameter (inch)	Outer Diameter (inch)	Position S/J	Orifice Angle	Bubble Size
1.	0.02	0.1875	S	30	5mm
2.	0.02	0.1875	S	45	5mm
3.	0.02	0.1875	J	30	2mm
4.	0.02	0.1875	J	60	2mm
5	0.01	0.1875	J	0	2mm
6.	0.005	0.1875	J	0	2mm

The double-walled tubes seemed to produce the same size bubbles irrespective of the angle in each position. The “J” position double-walled tubes produced a bubble of smaller radius. This is different from the hypothesis. Results from experiments conducted by Datta et al. were of this nature[17].

Orifice Angle

Double-walled tubes of varying orifice angles (0°, 30°, 45°, 60°) were tested. These were fabricated in the engineering workshop to have angular tips of 30°, 45°, 60° or flat-bottomed. It was hypothesized that the orifice angle should have no effect on the bubble size. The bubble interval should decrease with increase in angle.

Table 4 shows the effect of orifice angle on the bubble size. The results proved that the bubble size remained unaffected by the orifice angle. As seen in figure 23a, a higher angle shows lower bubble interval, hence higher bubble frequency in the “straight” position.

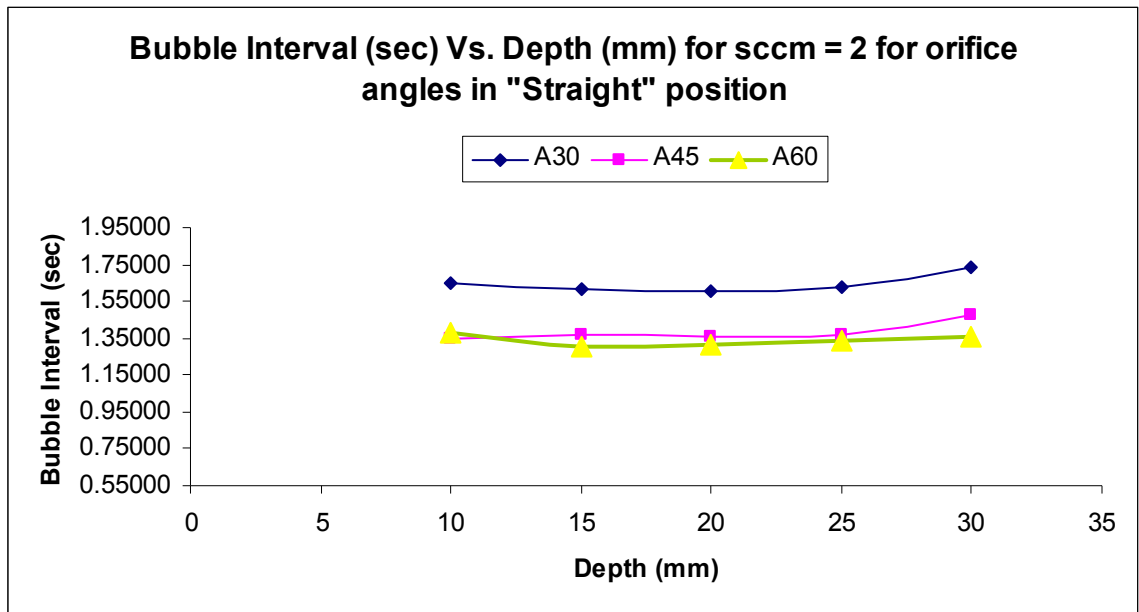


Figure 23a: Dependence of bubble interval on depth for straight position tube with orifice angles of 30°, 45° and 60°

Figure 23b shows the results for surface tension. The surface tension decreases as the orifice angle increases.

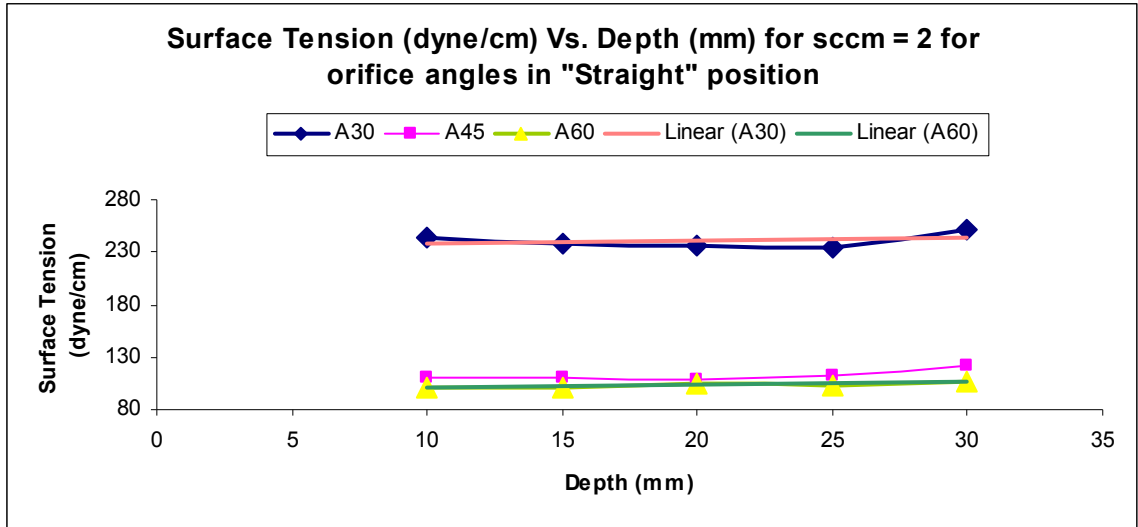


Figure 23b: Dependence of surface tension on depth for straight position tube with orifice angles of 30°, 45° and 60°

Depth

The depth was increased from 0 to 30 mm by rotating the spindle and thus lowering the capillary tube into the liquid to varying depths. A depth of 0mm corresponded to a reading at the surface. Measurements were taken at the following depths: 10mm, 15mm, 20mm, 25mm and 30mm. It was hypothesized that as the depth was increased, the offset pressure would increase due to increase in hydrostatic pressure. However, the change in voltage would remain almost constant as the total pressure of the system would remain constant due to increase in system pressure as well. Thus, the change in pressure would also remain constant. The following graphs show examples of the results from two capillary tubes.

The influence of bubble interval on depth is shown in figure 24a, offset voltage in 24b and change in volts in figure 24c. There seemed to be no significant change in bubble

interval or change in voltage or change in pressure due to increase in depth of immersion of the capillary irrespective of the flow rates.

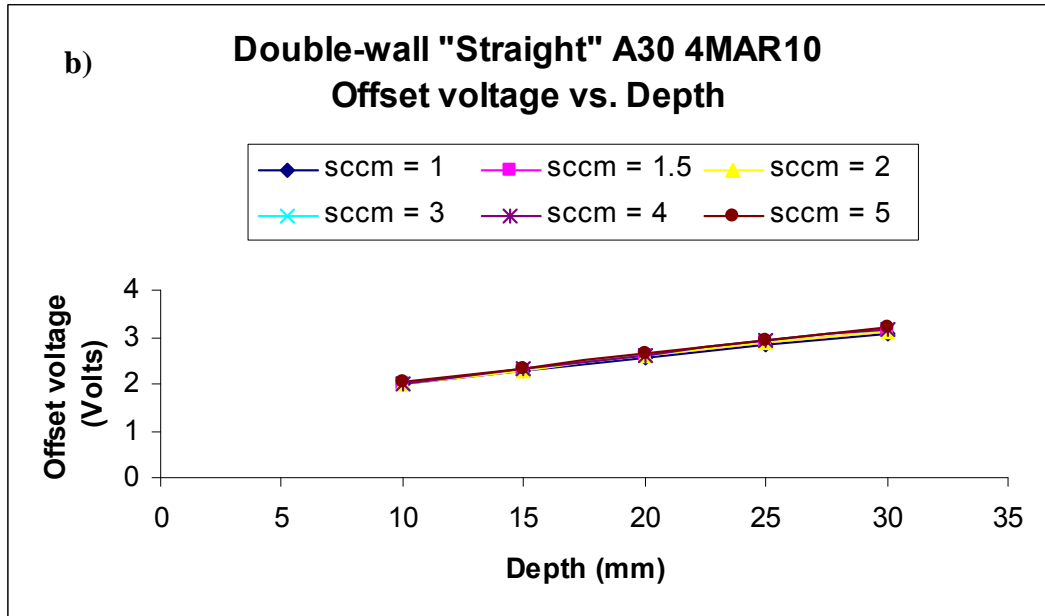
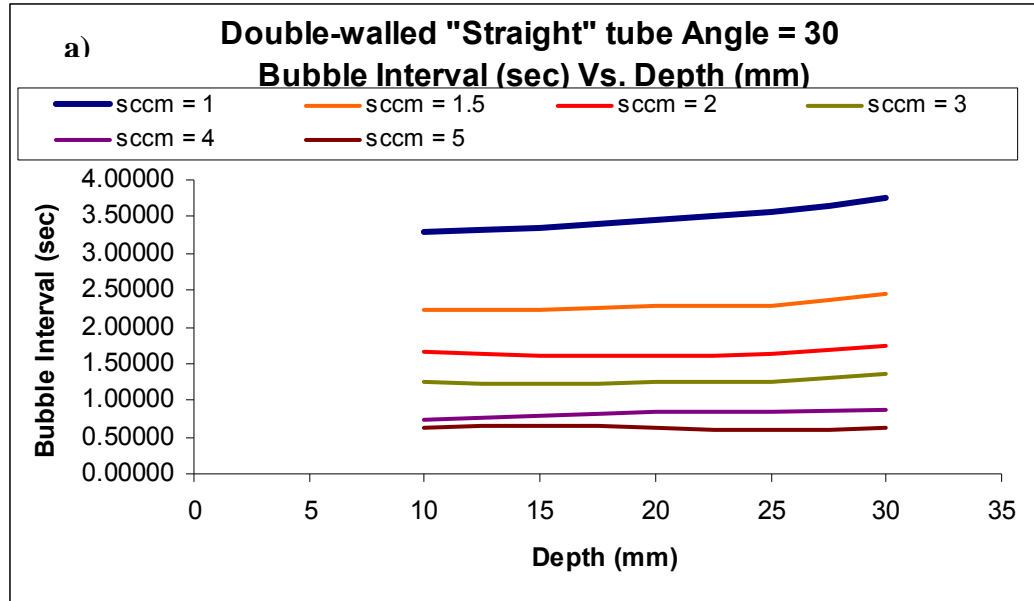


Figure 24: Effect of increasing depths on the a) Bubble Interval b) Offset voltage

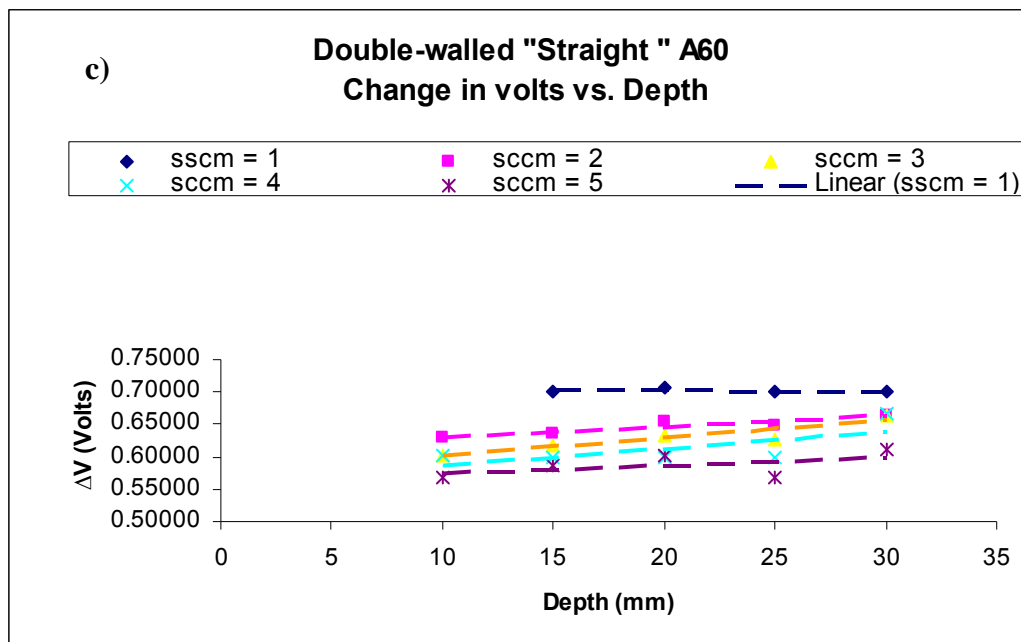


Figure 24c: Effect of increasing depths on change in volts

Flow Rate

The flow rate was varied from zero to five sccm in increments of 1 sccm. Readings were taken for 1, 2, 3, 4, 5 sccm values. A few readings for 1.5 sccm and higher flow rates were taken for oil measurements in the final analysis. The capillary tube was about 17cm in length and clamped to the depth measuring stand. The capillary tubes were made of electrochemically etched stainless steel on both the inner and outer sides.

With increase in flow rate, the bubble interval should reduce thus showing an increase in the bubble frequency for the same depth. From the results on depth, in figure 23b, since change in voltage decreases with increase in flow rate, change in pressure also decreases with increase in flow rate. Thus, surface tension should decrease with increase in flow rate. The experimental results for bubble interval in figure 25a, change in volts in

figure 25b and surface tension in figure 25c, prove that the results are in agreement with the hypothesis. However, according to literature, the surface tension should

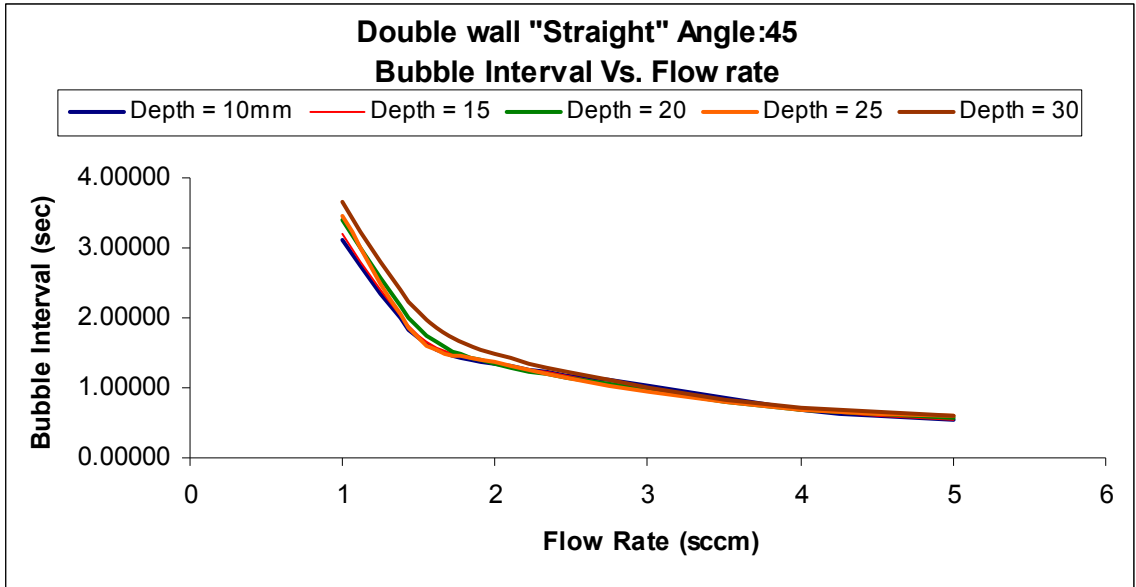


Figure 25a: “Straight” position: response of bubble interval to increasing flow rates

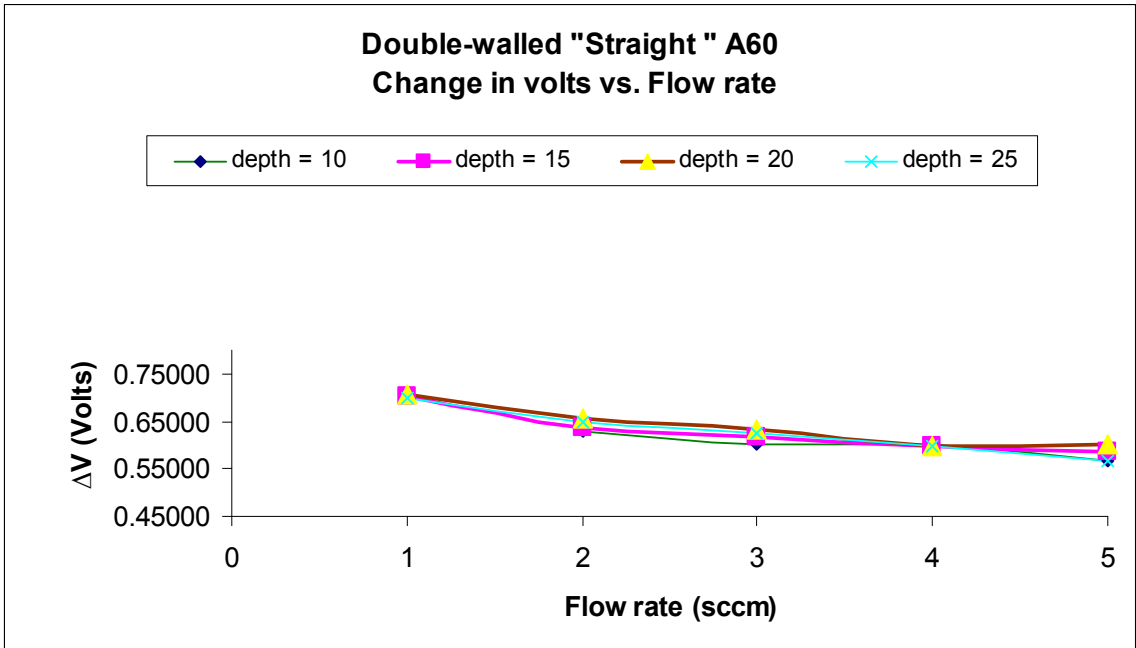


Figure 25b: “Straight” position: response of change in volts to increasing flow rates

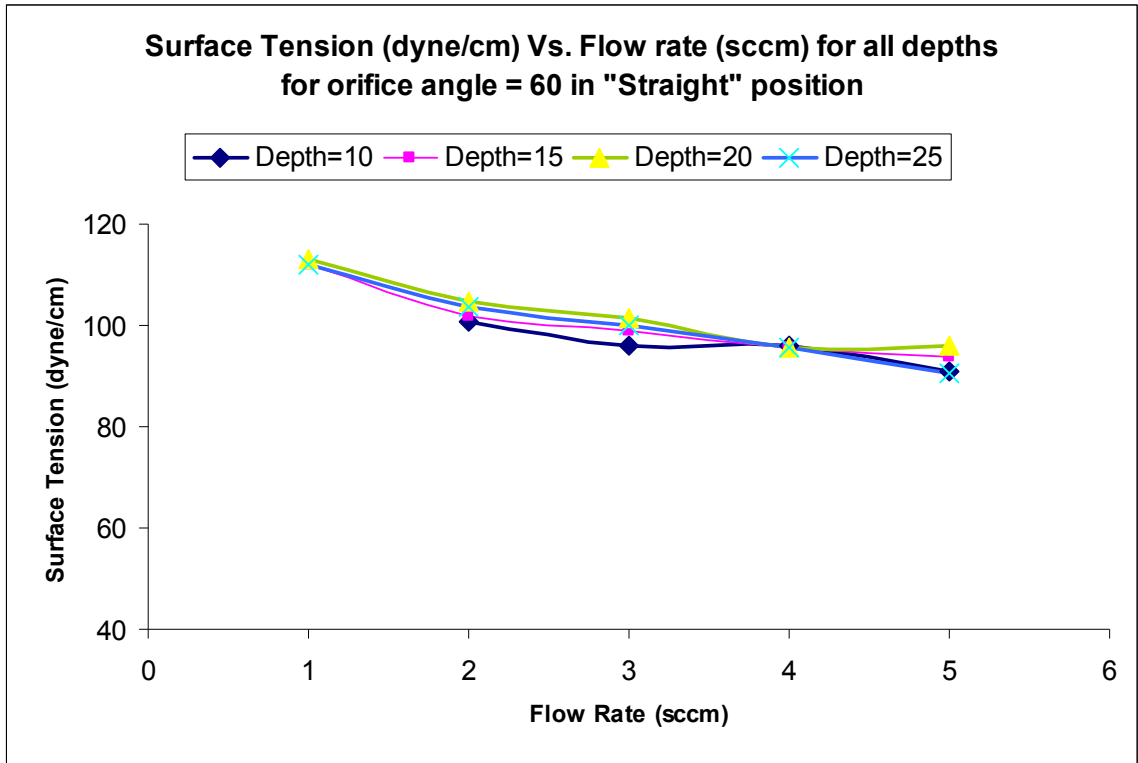


Figure 25c: Relation between Flow rate and Surface Tension of a double-walled tube in “straight” position

Figure 26 shows the relation between the change in pressure and surface tension. This is in agreement with the expected results from the Laplace equation.

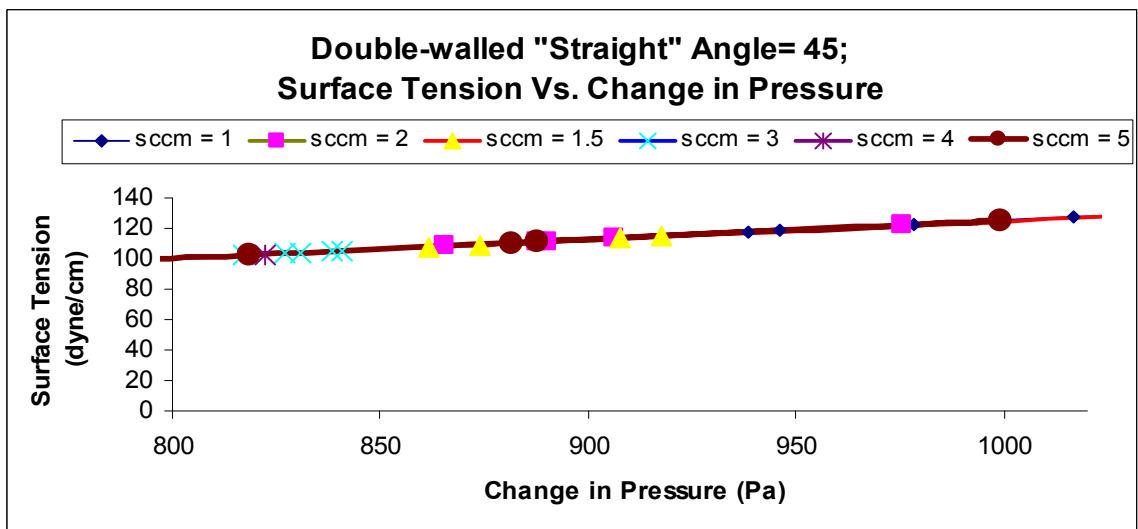


Figure 26: Relation between change in pressure and Surface Tension

A plot of surface tension vs. bubble lifetime would show the opposite trend as flow rate and bubble lifetime are inversely related (figure 27a).

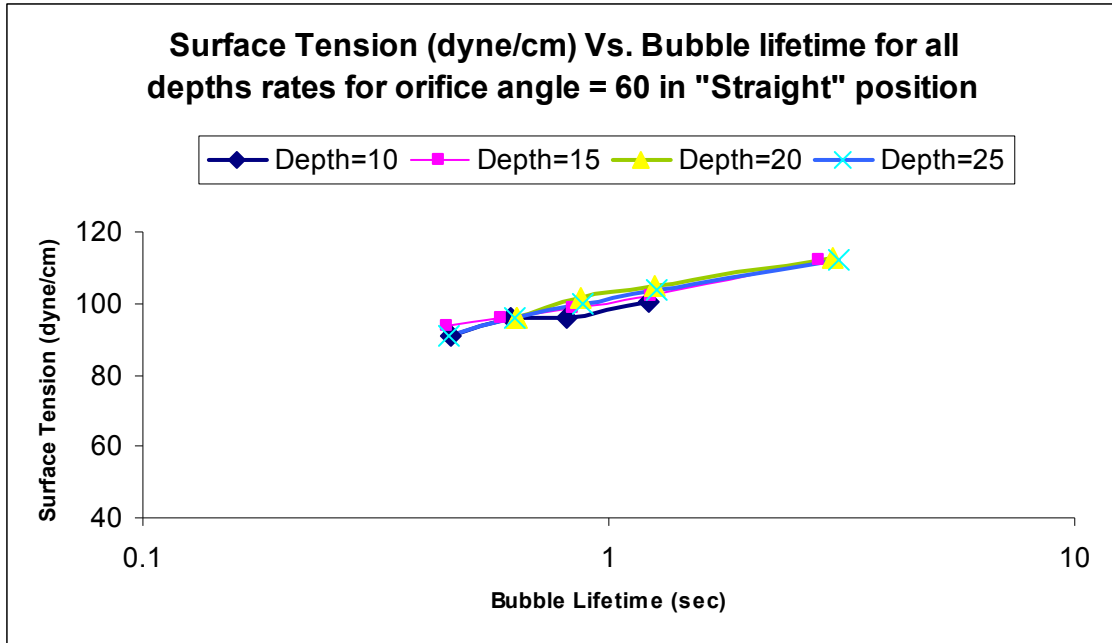


Figure 27a: Relation between surface tension and bubble lifetime

However, according to literature, (figure 27b), the trend should be opposite. The experiments conducted in this research, were over a very narrow range of 0.5 to 1.4 sec, while that in figure 27b are for a very large one. Efforts to increase this range or the bubble deadtime with various mass flow controllers or capillary tubes were unsuccessful. Reducing the flow rate to the very minimum value even did not show any significant difference. Capillaries of radii smaller than 0.005” may be a possible direction to take hereafter to study this aspect.

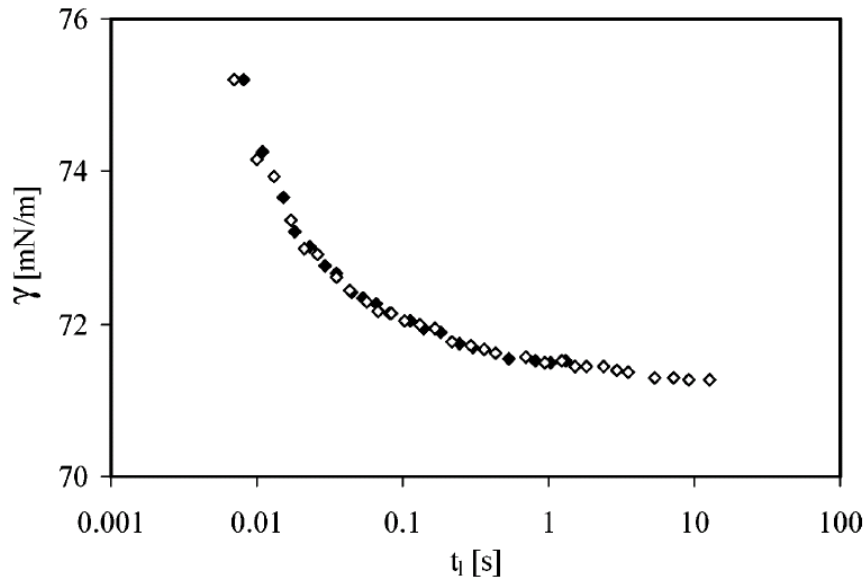


Figure 27b: Dependence of surface tension of pure water [8]

Figure 28 is a summary of the effect of depth and flow rates on the bubble interval in seconds and the volts. The capillary tube used in this case is a double-walled tube in the “straight” position with an orifice angle of 0° and inner diameter of 0.02”.

Orientation (Straight/Inverted)

The results presented so far were taken using a capillary tube in the “straight” position. The inverted or “J” shaped tube is a new structure proposed in this research as an alternative to introducing the capillary tube from the bottom of the liquid container. The construction of this tube is very simple; the end portion of the tube can be replaced easily with attachments of the straight or “J” shape holder thus making it easy to switch between the two configurations. The results presented below are a comparison of the results from the experiments conducted with the tubes in the two different positions.

Error! Objects cannot be created from editing field codes.

Figure 28: Relation between flow rates and depths with change in voltage for double-walled tube of orifice angle of 0°

The waveforms in the “J” position is hypothesized to show lower bubble intervals, as the bubbles face no restriction to being released due to any physical surface. Thus the surface tension should also be lower. Figure 29 confirms that the bubble interval of the “J” tube orientation is lower than the “Straight” tube orientation. The relation between surface tension and bubble interval in both orientation is seen in figure 30. The surface tension for the “J” tube orientation is lower; this implies that the “J” tube is less sensitive as change in volts must be lower. However, the value of surface tension is more accurate than in “Straight” position. This is due to the non-spherical nature of the bubbles in the “Straight” position. The radii of curvature in both x and y directions have to be considered, thereby resulting in a higher surface tension.

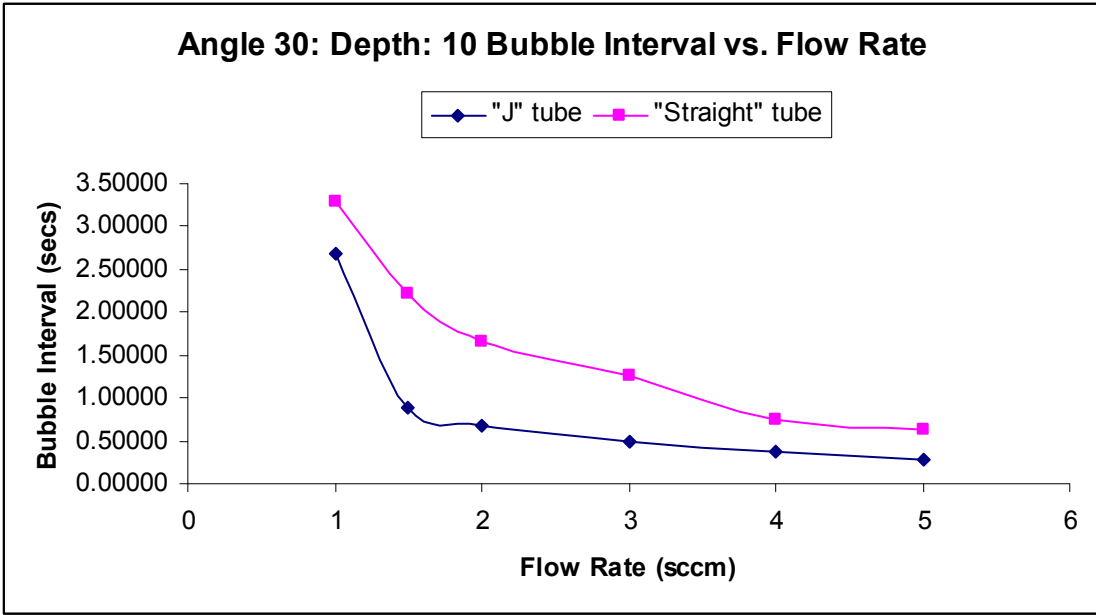


Figure 29: Bubble Interval Vs. Flow Rate for Straight and Inverted position for double-walled tube with an angle of 30° at the orifice

Table 5 contains some data showing the results for double-walled tubes with an angle of 30° in the two positions.

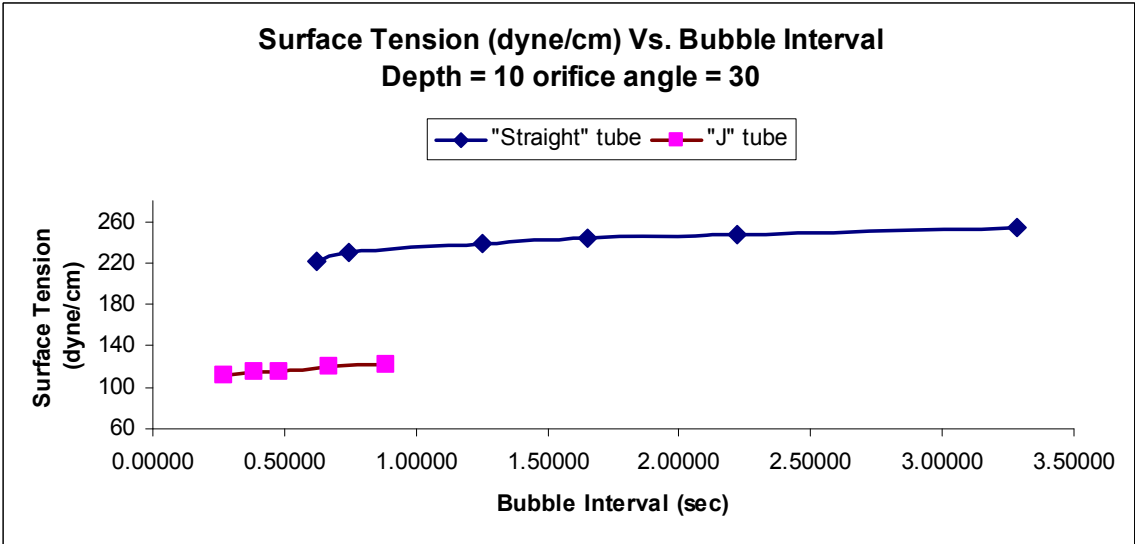


Figure 30: Relation between surface tension and bubble interval for “Straight” and “J” orientation

The above parameters were first tested in water and summarized as above. Based on the above results, double-walled tubes with an angle of 45° were selected for testing with glycerin and motor oil. Initial tests were conducted in water.

Table5: Bubble Interval information for different flow rates

Tube Position	Depth	Flow Rate (sccm)	Bubble Interval (s)	Bubble lifetime (s)	Bubble deadtime (s)
Straight 30°	10	1	3.28000	2.746	0.534
		2	1.65000	1.39	0.26
		3	1.25300	1.07	0.183
		4	0.74400	0.72	0.024
		5	0.62300	0.52	0.103
Inverted 30°	10	1	2.68000	2.58700	0.093
		2	1.48148	0.61700	0.054
		3	0.48000	0.40900	0.071
		4	0.38300	0.32100	0.062
		5	0.38300	0.22000	0.051

Table 6 summarizes the effects of all the parameters tested in this research work.

Table 6: Summary of the different parameters tested and their effects:

No.	Parameter	Effects
1.	Inner Diameter	Change in voltage increases with increase in internal diameter.
2.	Outer Diameter	Double-walled tubes seemed to produce the same size bubble irrespective of the angle in each position. The “J” position double-walled tubes produced a bubble of smaller radius.
3.	Single-walled / Double-walled	Single-walled tubes produced bubbles whose size was dependant on their inner diameter; double-walled tubes produced bubbles of the same size, depending on the orientation.
4.	Depth	Increasing depth resulted in an increase in offset voltage. Change in voltage/pressure, surface tension, and bubble interval for one flow rate remained unaffected.
5.	Flow rate	Higher flow rates showed an increase in bubble frequency; surface tension, bubble interval and change in pressure decreased with increase in flow rates.
6.	Orifice angle	Higher angles show a higher bubble frequency and lower surface tension.
7.	“Straight” / “J”	“Inverted” or “J” position has lower bubble interval.

4.2.2 Glycerin

Using the double-walled tube of 45° angular tip, the surface tension using equation and the viscosity were calculated using the formula provided for the Sensadyn tensiometer:

$$\Delta\gamma = 3\eta r/2B_1$$

where,

γ is the surface tension

η is the viscosity

r is the radius of the capillary tube orifice

B_1 is the bubble lifetime

The change in volts as a function of the flow rate (figure 31), decreases with increase in flow rate. The surface tension of glycerin was given as 63.1 dyne/cm at room temperature and the viscosity from calculations was in the range of 907.1 Pa.s to 1062.23 Pa.s. The corrected surface tension is in the range of 62.9 (i.e. 0.3% error) to 63.7 (0.95% error) dyne/cm. The average correction factor seems to be about 0.15.

Since glycerin has a much higher viscosity than water, the bubble interval range was expected to increase. Figure 32 shows the calculated surface tension of glycerin for different flow rates.

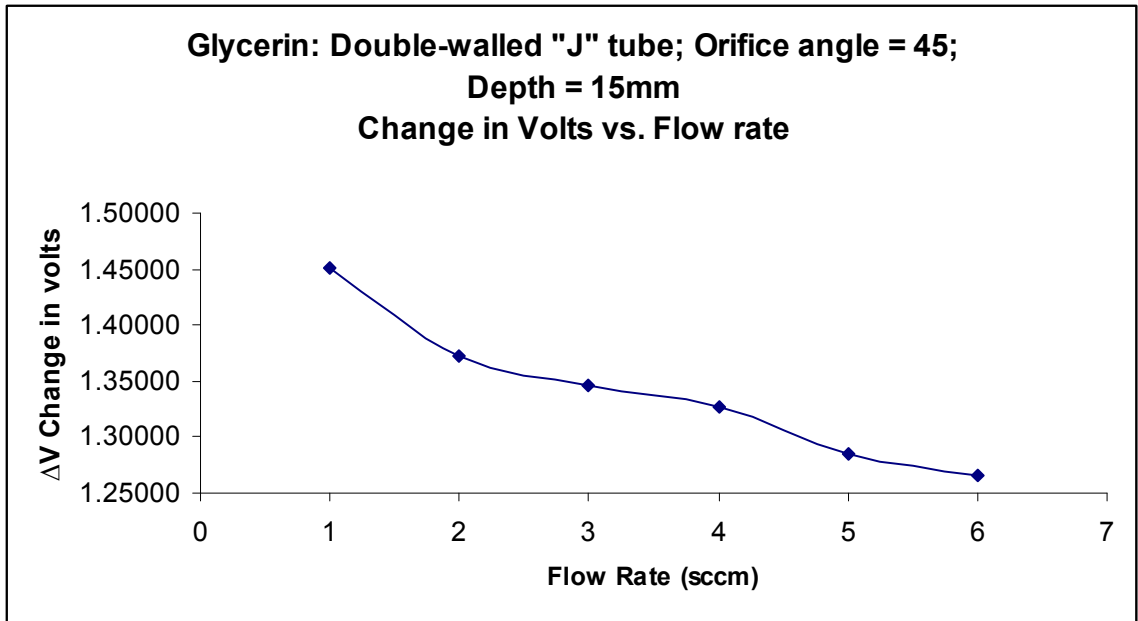


Figure 31: Relation between change in volts and the flow rate for glycerin using a double-walled “J” tube of orifice angle of 45°

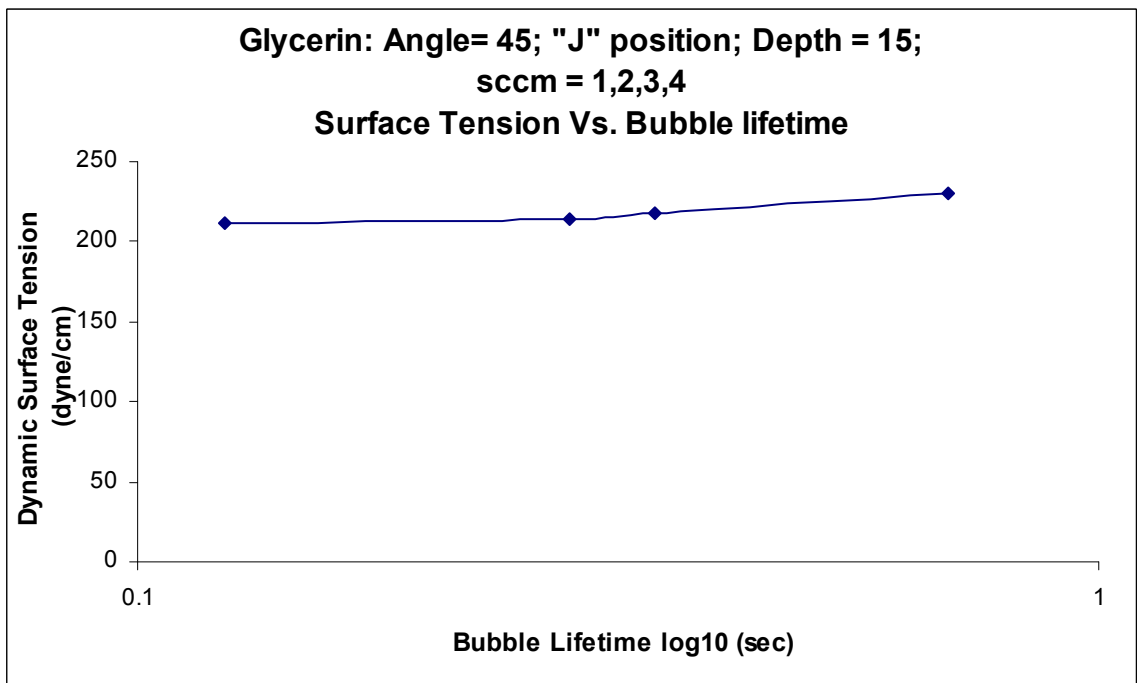


Figure 32: Relation between dynamic surface tension (dyne/cm) and bubble lifetime (s) for glycerin using a double-walled “J” tube of orifice angle of 45°

4.2.3 Motor Oil:

In order to verify our experiment, used Valvoline 10W30 motor oil was studied with clean oil of the same grade and brand. Both the surface tension and viscosity of the used oil were lower than that of the clean oil. However, the difference in viscosity was much higher. Figure 33 and 34, compare the surface tension and viscosity respectively, of used and clean motor oil. Both the surface tension and viscosity of the used oil was found to be lower than the clean one.

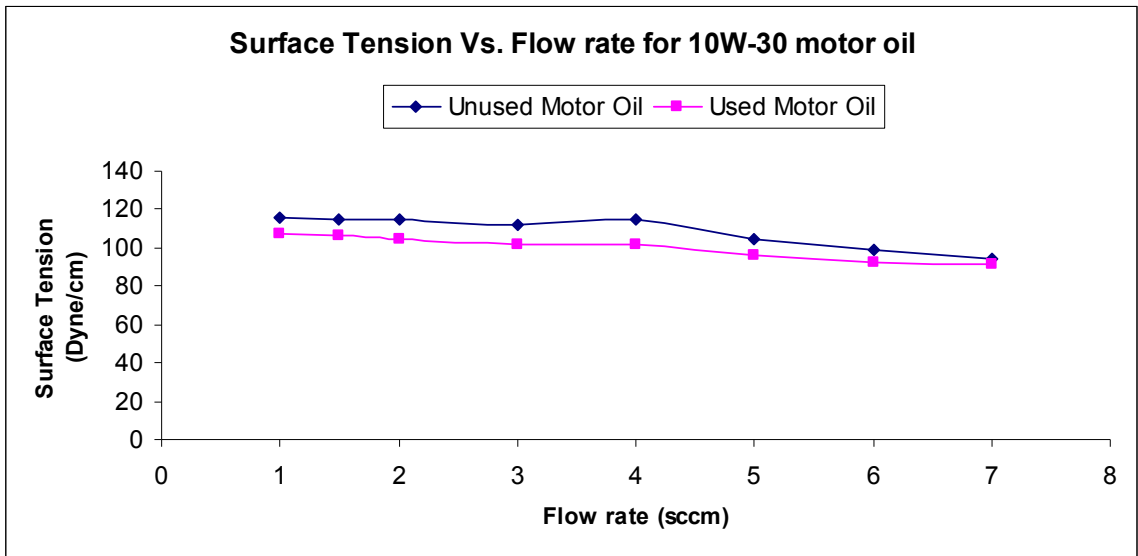


Figure 33: Surface tension of clean and used Valvoline 10W30 motor oil

The viscosity of both the oils, as measured using an Anton Paar – Physica MCR 301 viscometer, were in agreement with the experimental results; i.e. the viscosity of the used oil, was lower than that of the clean oil. The determining factor for viscosity change due to degradation would be the way the oil was used. Since oil degradation by subjection to high engine temperatures was difficult to achieve in a lab, used oil from an oil change

service station was used for experimental purposes. Both viscosity and surface tension were affected by degradation.

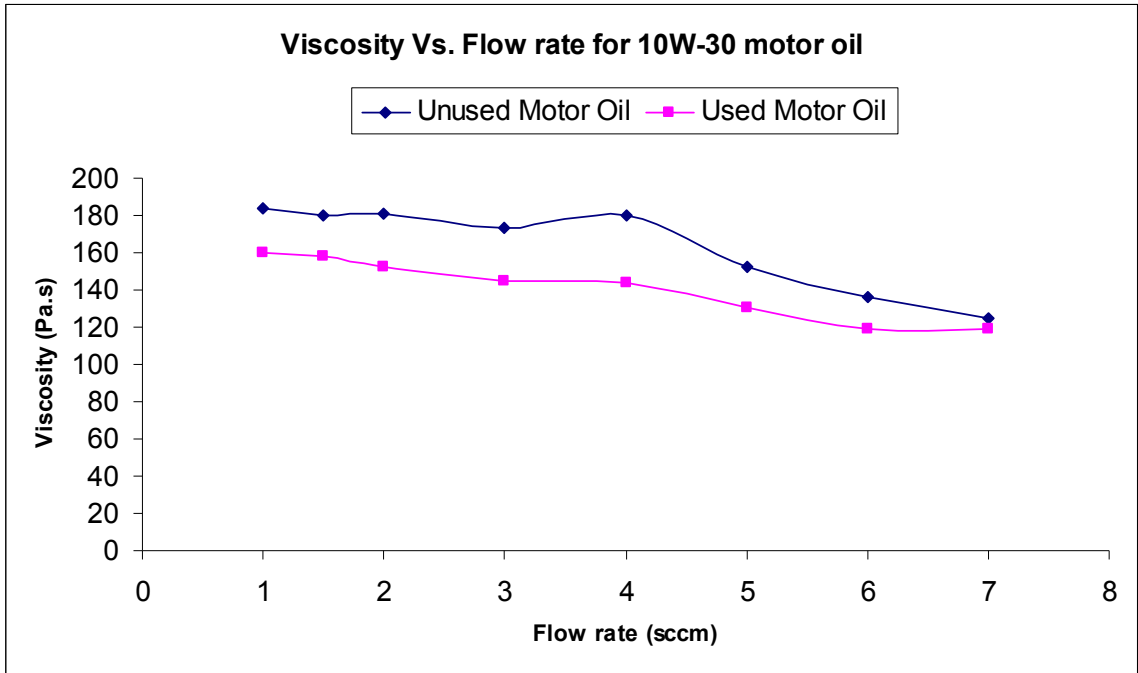


Figure 34: Viscosity of clean and used Valvoline 10W30 motor oil

Chapter 5. CONCLUSIONS

Using the Bubble Pressure method, an attempt to study the influence of various parameters such as orifice size, geometry of the tip of the capillary tube, geometry of the position of the tube, flow rates, and depths were studied. For a radius of 0.005", the results seemed to be erratic. A capillary tube of radius 0.02" or 0.25mm with a double-walled structure with an outer radius of 0.1875" and an angle of 30 degrees seemed to show improvements. Smaller radius tubes produced spherical bubbles of smaller size. Tubes were fabricated with a "J" or bent form to assist in release of bubbles. The bubble interval was much shorter in the inverted or "J" position.

The setup presented in this experiment is a simple and versatile one as the tubes can be inter-changed easily from "Straight" to "Inverted" position. The "J" orientation of the capillary tube eased the release and rise of bubbles.

Reference fluids like water and glycerin were used. Using the formulae given, the excess surface tension due to aerodynamic effects and the viscosity effects were calculated. By using the "J" orientation of the capillary tube, the calculated surface tension was much more accurate. On application of the formulae for corrections to surface tension, the corrected surface tension was very close to the actual value. By calculating the viscosity of clean and used Valvoline 10W-30 motor oil, it was possible to

detect the decrease in viscosity in the used oil. Both the surface tension and viscosity were affected by degradation.

REFERENCES

1. Samuel Sugden, "XCVII.—The determination of surface tension from the maximum pressure in bubbles", *J. of Chem. Soc. Trans.* 1922, 121, pp. 858-866
2. V.B. Fainerman, V.V.Mys, A.V. Makievski, R. Miller, "Application of the maximum bubble pressure technique for dynamic surface tension studies of surfactant solutions using the Sugden two-capillary method", *Journal of Colloid and Interface Science*, 2006, 304, pp. 222-225
3. Fainerman, V. B.; Kazakov, V. N.; Lylyk, S.V.; Makievski, A.V ; Miller, R., "Dynamic surface tension measurements of surfactant solutions using the maximum bubble pressure method – limits of applicability", *Colloids and Surfaces A: Physiochem. Eng. Aspects*, 2004, 250, pp. 97-102
4. Fainerman V.B., Miller R., "Maximum bubble pressure tensiometry- an analysis of experimental constraints", *Advances in Colloid and Interface Science*, 2004, 108-109, pp. 287-301
5. Fainerman, V. B.; Miller, R., "The maximum bubble pressure technique, monograph in Drops and Bubbles in Interfacial Science", in: Möbius, D., Miller, R. (Eds.), *Studies of Interface Science*; Elsevier: Amsterdam, 1998, Vol 6, pp. 279-326
6. Mysels, Karol J., "Improvements in the maximum-Bubble-Pressure Method of Measuring Surface Tension", *Langmuir* 2, 1986, Vol 2 (4), pp. 428-432

7. Kovulchuk, V.I.;Dukhin,.S. S. Colloids Surf., 2001, A 192, 131
8. Fainerman, V.B.; Mys, V.D.; Makievski, A.V.; Miller, R, “Correction for the Aerodynamic Resistance and Viscosity in Maximum Bubble Pressure Tensiometry”, Langmuir, 2004, 20, 1721-1723
9. http://en.wikipedia.org/wiki/Maximum_bubble_pressure_method
10. Fainerman, Makievski and Miller, “Accurate analysis of the bubble formation process in maximum bubble pressure tensiometry”, Review of scientific instruments, Jan 2004, Vol 75, No.1, pp. 213-221
11. http://www.lauda.de/hosting/lauda/website_en.nsf/urlnames/mptc_anwendungen
12. “Dynamic Surface Tension Determining the surface tension of surfactants in aqueous solutions made easy”, April 2002 Laboratory News for SITA pro line f10
13. Livingstone Greg J., Thompson Brian T., Wooton Dave, “Determining the root causes of fluid degradation utilizing oil analysis in Root Cause Analysis in Practising Oil Analysis”, January – February 2007, pp. 36-43
14. Handbook of Chemistry and Physics, 90th edition, 2009-2010
15. Accurate analysis of the bubble formation process in maximum bubble pressure tensiometry, Fainerman, makievski and Miller, Review of scientific instruments, Vol 75 No.1, Jan 2004, pp 213-221
16. Liow, Jong-Leng, “Quasi-equilibrium bubble formation during top-submerged gas injection”, Chemical Engineering Science, 2000, Vol 55, pp. 4515-4524
17. Datta, R. L., Napier, D. H., & Newitt, D. M., “The properties and behaviour of gas bubbles formed at a circular orifice”, Transactions of the Institution of Chemical Engineers, 1950, 28, 14-26

18. R. Defay and I. Prigogine: Surface Tension and Adsorption (Longmans, Green & Co., London, 1966)
19. Fainerman V. B., Makievski A. V., Miller R, “The measurement of dynamic surface tensions of highly viscous liquids by the maximum bubble pressure method” , Colloids and Surfaces A: Physicochemical and Engineering Aspects, 1993, 75, pp. 229-235
20. Perry’s Chemical Handbook

Appendix A: CORRECTION FACTORS FOR DOUBLE-WALL TUBES

1. Correction factors for double-walled capillary tube in “straight” position for orifice angle = 30° in water

sccm	Depth	ΔV	Bubble Interval	ΔP	Corr_F	BD	BL
1	10	0.79540	3.28000	2031.672	0.283392	0.534	2.74600
	15	0.77630	3.34000	1983.256	0.29031	1.27	2.07000
	20	0.80130	3.44300	2046.627	0.281321	0.534	2.90900
	25	0.79840	3.57700	2039.276	0.282335	0.443	3.13400
	30	0.72660	3.75000	1857.275	0.310003	0.48	3.27000
1.5	10	0.772	2.22300	1972.357	0.291915	0.166	2.05700
	15	0.75830	2.23000	1937.629	0.297147	0.167	2.06300
	20	0.75980	2.27300	1941.432	0.296565	0.166	2.10700
	25	0.76030	2.27300	1942.699	0.296371	0.166	2.10700
	30	0.80860	2.45000	2065.132	0.278801	0.17	2.28000
2	10	0.7612	1.65000	1944.98	0.296024	0.26	1.39000
	15	0.74270	1.61300	1898.086	0.303337	0.307	1.30600
	20	0.74170	1.60300	1895.551	0.303743	0.123	1.48000
	25	0.73490	1.63000	1878.314	0.30653	0.117	1.51300
	30	0.78520	1.73300	2005.816	0.287045	0.136	1.59700
3	10	0.74950	1.25300	1915.323	0.300607	0.183	1.07000
	15	0.71920	1.23000	1838.517	0.313165	0.127	1.10300
	20	0.71340	1.26300	1823.815	0.31569	0.166	1.09700
	25	0.71970	1.26000	1839.785	0.31295	0.16	1.10000
	30	0.77340	1.36000	1975.905	0.29139	0.16	1.20000
4	10	0.71970	0.74400	1839.785	0.31295	0.024	0.72000
	15	0.69730	0.80000	1783.004	0.322916	0.11	0.69000
	20	0.68700	0.84000	1756.895	0.327714	0.117	0.72300
	25	0.69280	0.83300	1771.597	0.324995	0.11	0.72300
	30	0.75290	0.88000	1923.941	0.299261	0.1	0.78000
5	10	0.69430	0.62300	1775.4	0.324299	0.103	0.52000
	15	0.70460	0.64400	1801.509	0.319599	0.094	0.55000
	20	0.67090	0.61400	1716.085	0.335508	0.09	0.52400
	25	0.65770	0.61000	1682.625	0.34218	0.084	0.52600
	30	0.68160	0.63700	1743.207	0.330288	0.09	0.54700

2. Correction factors for double-walled capillary tube in “straight” position for orifice angle = 45° in water

sccm	Depth	ΔV	Bubble_Interval	ΔP (Pa)	Corr_F	BD	BL
1	10	0.73430	3.11600	938.3966	0.613557	0.173	2.94300
	15	0.74030	3.20700	946.0011	0.608625	0.173	3.03400
	20	0.76570	3.39300	978.1935	0.588595	0.337	3.05600
	25	0.79590	3.45400	1016.47	0.566431	0.317	3.13700
	30	0.83490	3.66000	1065.899	0.540164	0.344	3.31600
1.5	10	0.6836	1.71400	874.1385	0.65866	0.137	1.57700
	15	0.71000	1.73700	907.5983	0.634378	0.127	1.61000
	20	0.71780	1.85600	917.4842	0.627542	0.196	1.66000
	25	0.67390	1.71000	861.8445	0.668056	0.14	1.57000
	30	0.80960	2.09700	1033.833	0.556918	0.18	1.91700
2	10	0.6963	1.34300	890.2347	0.646751	0.103	1.24000
	15	0.69440	1.37000	887.8266	0.648505	0.123	1.24700
	20	0.67680	1.35300	865.52	0.665219	0.133	1.22000
	25	0.70900	1.37300	906.3309	0.635265	0.11	1.26300
	30	0.76360	1.48000	975.532	0.590201	0.123	1.35700
3	10	0.65530	1.02000	838.2705	0.686843	0.11	0.91000
	15	0.64940	0.98000	830.7928	0.693025	0.09	0.89000
	20	0.64650	0.98300	827.1173	0.696104	0.1	0.88300
	25	0.63870	0.94000	817.2314	0.704525	0.08	0.86000
	30	0.65720	1.00700	840.6786	0.684875	0.097	0.91000
4	10	0.60250	0.68000	771.3508	0.746431	0.096	0.58400
	15	0.60160	0.68300	770.2102	0.747536	0.08	0.60300
	20	0.60350	0.69600	772.6183	0.745206	0.093	0.60300
	25	0.62400	0.69000	798.6003	0.720961	0.084	0.60600
	30	0.64250	0.70700	822.0476	0.700397	0.09	0.61700
5	10	0.61330	0.54700	785.039	0.733416	0.077	0.47000
	15	0.63970	0.55600	818.4988	0.703434	0.08	0.47600
	20	0.69430	0.58400	887.6999	0.648598	0.08	0.50400
	25	0.78220	0.60300	999.1059	0.576275	0.09	0.51300
	30	0.68950	0.59600	881.6163	0.653073	0.073	0.52300

3. Correction factors for double-walled capillary tube in “straight” position for orifice angle = 60 ° in water

sccm	Depth	ΔV	Bubble Interval	ΔP	Corr_F	BD	BL
1	15	0.70120	3.27400	896.445	0.64227	0.447	2.82700
	20	0.70710	3.38300	903.9228	0.636957	0.366	3.01700
	25	0.70020	3.48000	895.1776	0.64318	0.37	3.11000
	30	0.69930	3.40000	894.037	0.644	0.29	3.11000
2	10	0.6289	1.38400	804.8107	0.715398	0.167	1.21700
	15	0.63680	1.30000	814.8233	0.706607	0.064	1.23600
	20	0.65430	1.32000	837.0031	0.687883	0.07	1.25000
	25	0.64840	1.34000	829.5254	0.694084	0.07	1.27000
	30	0.66410	1.35400	849.4238	0.677824	0.067	1.28700
3	10	0.60060	0.87300	768.9428	0.748768	0.06	0.81300
	15	0.61720	0.90400	789.9819	0.728827	0.067	0.83700
	20	0.63380	0.94000	811.021	0.70992	0.07	0.87000
	25	0.62590	0.95000	801.0084	0.718794	0.067	0.88300
	30	0.66510	0.97300	850.6912	0.676814	0.063	0.91000
4	10	0.60050	0.67400	768.816	0.748892	0.06	0.61400
	15	0.59860	0.65300	766.4079	0.751245	0.066	0.58700
	20	0.59860	0.69300	766.4079	0.751245	0.06	0.63300
	25	0.59860	0.69300	766.4079	0.751245	0.063	0.63000
	30	0.66700	0.78300	853.0993	0.674904	0.07	0.71300
5	10	0.56830	0.52000	728.0051	0.790874	0.063	0.45700
	15	0.58690	0.51300	751.5791	0.766067	0.063	0.45000
	20	0.60060	0.69400	768.9428	0.748768	0.06	0.63400
	25	0.56640	0.51300	725.597	0.793498	0.06	0.45300
	30	0.61130	0.55400	782.5041	0.735792	0.064	0.49000

4. Correction factors for double-walled capillary tube in “J” position for orifice angle = 45° in Glycerin

sccm	Depth	ΔV	Bubble Interval	ΔP	Corr_F	BD	BL
1	15	1.45020	5.51300	1845.741	0.31194	0.54	4.973
2		1.37210	2.70000	1746.756	0.329617	0.4816	2.2184
3		1.34660	2.17330	1714.437	0.33583	0.2633	1.91
4		1.3261	1.56170	1688.455	0.340998	0.2334	1.3283
5		1.28510	1.23500	1636.491	0.351826	0.2383	0.9967
6		1.26660	1.04000	1613.043	0.35694	0.2166	0.8234

5. Correction factors for double-walled capillary tube in “J” position for orifice angle = 45° in clean Valvoline 10W-30 motor oil

sccm	Depth	ΔV	Bubble Interval	ΔP	Corr_F	BD	BL
1	10	0.36919	1.68700	951.2989	0.605236	0.075	1.612
1.5		0.35399	0.90500	912.7694	0.630784	0.067	0.838
2		0.34914	0.72900	900.4754	0.639396	0.066	0.663
3		0.35011	0.55900	902.9342	0.637654	0.059	0.5
4		0.33449	0.41300	863.3401	0.666898	0.063	0.35
5		0.32425	0.32500	837.3833	0.68757	0.058	0.267
6		0.31352	0.26700	810.1845	0.467647	0.054	0.213
7		0.30618	0.22600	791.5788	0.478638	0.054	0.172
1	15	0.36040	1.69600	929.0177	0.407829	0.146	1.55
1.5		0.35600	0.90900	917.8644	0.412784	0.084	0.825
2		0.35740	0.73300	921.4132	0.411194	0.063	0.67
3		0.34810	0.56200	897.8392	0.421991	0.062	0.5
4		0.3569	0.42500	920.1458	0.411761	0.063	0.362
5		0.32320	0.31700	834.7218	0.4539	0.055	0.262
6		0.30470	0.26200	787.8273	0.480918	0.054	0.208
7		0.29150	0.22100	754.3674	0.502249	0.058	0.163
1	20	0.36230	1.23400	933.8339	0.616555	0.08	1.154
1.5		0.35740	0.91700	921.4132	0.624866	0.075	0.842
2		0.38080	0.73300	980.7284	0.587074	0.062	0.671
3		0.35160	0.56700	906.7111	0.634998	0.075	0.492
4		0.40290	0.50000	1036.748	0.555352	0.071	0.429
5		0.31590	0.31300	816.2175	0.7054	0.071	0.242
6		0.29690	0.25900	768.0556	0.749633	0.055	0.204
7		0.28510	0.21200	738.1445	0.78001	0.05	0.162

6. Correction factors for double-walled capillary tube in “J” position for orifice angle = 45° in used Valvoline 10W-30 motor oil

sccm	Depth	ΔV	Bubble Interval	ΔP	Corr_F	BD	BL
1	15	0.33254	1.11330	858.3971	0.441381	0.0566	1.0567
1.5		0.33102	0.78330	854.5442	0.443371	0.0533	0.73
2		0.32425	0.62000	837.3833	0.452457	0.0533	0.5667
3		0.31497	0.45170	813.8601	0.465535	0.0484	0.4033
4		0.31351	0.34000	810.1592	0.467661	0.0483	0.2917
5		0.29740	0.25500	769.323	0.492485	0.0517	0.2033
6		0.28410	0.21170	735.6096	0.515056	0.0417	0.17
7		0.28370	0.18000	734.5957	0.515767	0.045	0.135